INSTITUTO POLITÉCNICO DE BRAGANÇA
Escola Superior de Tecnologia e Gestão

FIRE INSULATION PERFORMANCE OF NON-LOAD BEARING LSF WALLS

Rami Regaig

This thesis is submitted to the School of Technology and Management at the Polytechnic Institute of Bragança in partial fulfilment of the requirements for the Master of Science degree in Construction Engineering.

Supervised by:

Prof. Paulo Alexandre Gonçalves Piloto

Bragança

May 2024

Acknowledgement

I am deeply grateful to the esteemed faculty at IPB for their unwavering support, insightful feedback, and dedication to fostering academic excellence. Their commitment to excellence has been a constant source of inspiration throughout my master's thesis journey. I extend my heartfelt appreciation to my supervisor, Paulo Piloto, for their exceptional mentorship, invaluable guidance, and unwavering support.

Their expertise, patience, and encouragement have been instrumental in shaping this research and helping me navigate the complexities of my study. I am truly fortunate to have had the opportunity to learn from such esteemed professionals.

Abstract

This study looks at the fire insulation performance of non-load bearing light steel frame (LSF) walls, which are critical for guaranteeing the safety and resilience of modern building constructions. Understanding the behavior of LSF systems under fire circumstances is critical as they become more widely used in construction. The study process comprises the evaluation of experimental testing of several LSF wall constructions under common fire scenarios, followed by a thorough examination of thermal performance, structural integrity, and fire resistance ratings. The results show that LSF walls have promising fire insulation qualities, with insulating material, wall assembly design, and fastening techniques all having a major impact on performance. Furthermore, the findings emphasize the necessity of suitable installation techniques and fire-rated materials in improving the overall fire resistance of LSF wall systems. These ideas help to advance construction.

These findings help advance building design methods, code development, and fire safety standards in the construction sector, eventually fostering the production of more resilient and secure built environments.

A numerical model was developed to validate the full-scale fire test results. The insulation criterion, defined by the average or maximum temperature on the unexposed side of the wall, was evaluated. Additionally, 2D numerical analyses explored the thermal effects of cavity size and protection layers. The research highlights the impact of cavity insulation and offers insights into enhancing fire resistance for LSF walls.

ANSYS Multiphysics software is used for numerical validation and parametric analysis, demonstrating the influence of structural stud spacing, cavity thickness and protective layers.

The results indicate that cavity insulation has the largest impact on fire resistance for insulation, followed by increasing the number of gypsum plasterboards in the protective layer. Reducing stud spacing in walls and increasing the cavity thickness improves the fire resistance.

Résumé

Cette étude examine la performance en matière d'isolation au feu des murs en ossature légère en acier (LSF) non porteurs, qui sont essentiels pour garantir la sécurité et la résilience des constructions modernes. Comprendre le comportement des systèmes LSF en cas d'incendie est crucial alors qu'ils sont de plus en plus utilisés dans la construction. Le processus d'étude comprend l'évaluation des essais expérimentaux de plusieurs constructions murales LSF dans des scénarios d'incendie courants, suivie d'un examen approfondi de la performance thermique, de l'intégrité structurelle et des classements de résistance au feu.

Les résultats montrent que les murs LSF présentent des qualités prometteuses en matière d'isolation au feu, avec des matériaux isolants, une conception d'assemblage murale et des techniques de fixation ayant tous un impact majeur sur la performance. De plus, les conclusions soulignent la nécessité de techniques d'installation appropriées et de matériaux ignifuges pour améliorer la résistance au feu globale des systèmes de murs LSF.

Ces idées contribuent à faire progresser la construction. Ces conclusions contribuent à faire progresser les méthodes de conception des bâtiments, le développement des codes et les normes de sécurité incendie dans le secteur de la construction, favorisant finalement la production d'environnements construits plus résilients et sécurisés. Un modèle numérique a été développé pour valider les résultats des essais au feu à grande échelle. Le critère d'isolation, défini par la température moyenne ou maximale du côté non exposé du mur, a été évalué. De plus, des analyses numériques en 2D ont exploré les effets thermiques de la taille de la cavité et des couches de protection. La recherche met en évidence l'impact de l'isolation de la cavité et offre des perspectives pour améliorer la résistance au feu des murs LSF.

Le logiciel ANSYS Multiphysics est utilisé pour la validation numérique et l'analyse paramétrique, démontrant l'influence de l'espacement des montants structurels, de l'épaisseur de la cavité et des couches de protection. Les résultats indiquent que l'isolation de la cavité a le plus grand impact sur la résistance au feu pour l'isolation, suivi de l'augmentation du nombre de plaques de plâtre dans la couche de protection. Réduire l'espacement des montants dans les murs et augmenter l'épaisseur de la cavité améliore la résistance au feu

RESUMO

Esta pesquisa analisa o desempenho de isolamento ao fogo de paredes de estrutura de aço leve não portadoras de carga (LSF), que são fundamentais para garantir a segurança e a resiliência das construções modernas. Compreender o comportamento dos sistemas LSF em situações de incêndio é crucial à medida que são cada vez mais utilizados na construção. O processo de estudo envolve a avaliação de testes experimentais de várias construções de parede LSF em cenários de incêndio comuns, seguida por uma análise minuciosa do desempenho térmico, integridade estrutural e classificações de resistência ao fogo.

Os resultados mostram que as paredes LSF têm qualidades promissoras de isolamento ao fogo, com materiais isolantes, design de montagem de parede e técnicas de fixação tendo um impacto significativo no desempenho. Além disso, as descobertas enfatizam a necessidade de técnicas de instalação adequadas e materiais com classificação de fogo para melhorar a resistência geral ao fogo dos sistemas de paredes LSF.

Essas ideias ajudam a avançar na construção. Essas descobertas ajudam a avançar nos métodos de projeto de construção, desenvolvimento de códigos e padrões de segurança contra incêndio no setor da construção, eventualmente promovendo a produção de ambientes construídos mais resilientes e seguros. Um modelo numérico foi desenvolvido para validar os resultados dos testes de incêndio em escala real. O critério de isolamento, definido pela temperatura média ou máxima no lado não exposto da parede, foi avaliado. Além disso, análises numéricas 2D exploraram os efeitos térmicos do tamanho da cavidade e camadas de proteção. A pesquisa destaca o impacto do isolamento da cavidade e oferece insights para aprimorar a resistência ao fogo das paredes LSF.

O software ANSYS Multiphysics é usado para validação numérica e análise paramétrica, demonstrando a influência do espaçamento das vigas estruturais, espessura da cavidade e camadas de proteção. Os resultados indicam que o isolamento da cavidade tem o maior impacto na resistência ao fogo para isolamento, seguido pelo aumento do número de placas de gesso na camada de proteção. Reduzir o espaçamento das vigas nas paredes e aumentar a espessura da cavidade melhora a resistência ao fogo.

Index

List of figures

List of tables

Notation

Latin Lower Case Letters

h: ˙ Heat flux [W/m2]

p: Pressure [MPa]

t: Time [s]

Cp Specific heat at constant pressure [kJ/(kg K)]

Kxx,yy,zz: Thermal conductivity in x,y,z directions [W/mK]

Q: rate of heat transfer

Ts: the surface temperature

T∞: the fluid temperature

V~: Velocity vector [m/s]

Greek Letters

εm: Surface Emissivity of Member [a dimensional]

εf: Emissivity of the fire [a dimensional]

σ: Stephan Boltzmann constant = 5, 67 × 10−8 [W/m2K4]

λ: Thermal conductivity [kW/(m◦C)] ρ Density [kg/m3]

ρ: Density [kg/m3]

ρ0: Specific Mass [kg/m3]

T: Temperature

dT/dx: the temperature gradient [K/m].

Acronyms

(FRR): fire resistance ratings.

(E): The assessment of integrity.

(HF): Hot Flange.

(CF): Cold Flange.

(FEA).: finite element analysis.

(RMSE): Root Mean Square Error

T_{AVG} :(average temperature of the unexposed surface).

T_{MAX} :(maximum temperature of the unexposed surface).

(CFD): Computational Fluid Dynamics

(HRR): Heat Release Rate

(PPE): Personal Protective Equipment

(UV): Ultraviolet Radiation

(IR): Infrared Radiation

Chapter 1

1- INTRODUCTION

The fire insulation performance of non-load bearing LSF walls encompasses their ability to withstand heat transfer and maintain structural integrity in the event of a fire. These walls, which bear no vertical loads beyond their own weight, are commonly employed as partitions or cladding elements within buildings. Light steel framing (LSF) stands as a construction method utilizing cold-formed steel sections (CFS) as the primary structural elements, known for its versatility and efficiency in modern building practices.

The determination of fire insulation performance in non-load bearing LSF walls involves a multitude of factors. Key considerations include the composition and dimensions of the steel sections used, the configuration and number of plasterboard layers lining the walls, the type and positioning of insulation materials, as well as the dimensions and geometry of the wall cavity. Additionally, the performance is influenced by the specific conditions of fire exposure and scenario, including temperature, and duration.

Understanding and optimizing the fire insulation performance of non-load bearing LSF walls requires a comprehensive assessment of these factors. This involves meticulous selection and integration of materials, meticulous design considerations, and adherence to fire safety standards and regulations. By addressing these elements, designers and engineers can enhance the fire resilience of LSF walls, contributing to overall building safety and longevity.

1.1- Objective

The study investigates the fire resistance of LSF non-load bearing walls, aiming to provide insights into enhancing their fire performance. The experimental tests were developed to validate the numerical models., focusing on the insulation criterion defined by the average or maximum temperature on the unexposed side of the wall. The primary goal is to assess how LSF walls perform under fire conditions, emphasizing the importance of non-load bearing walls in partitioning spaces within a building.

Further investigation into cavity size revealed that larger cavities tend to enhance fire resistance, while consideration of different plasterboard lining configurations showed that external insulation surprisingly outperformed cavity insulation in terms of thermal protection.

To compare numerical simulations with experimental results, two types of errors were used: Relative Error to assess fire resistance time and Root Mean Square Error (RMSE) to analyse temperature errors during the simulation at specific points across the wall section. This comprehensive analysis offers valuable insights for optimizing fire resistance in LSF walls.

1.2- LSF Constructions and its history

LSF, short for light steel framing, revolutionizes building construction by utilizing cold-formed steel sections as primary structural components. The construction of LSF walls involves steel studs and sheathing boards, such as plasterboard or oriented strand board, forming the framework. These walls can serve as load-bearing or non-load-bearing structures, depending on whether they support vertical loads beyond their own weight.

The emergence of LSF walls gained significant traction during the Second World War, driven by the urgent need for rapid and cost-effective construction of both temporary and permanent structures. Innovations such as self-drilling screws, prefabricated panels, and advancements in fire resistance and thermal insulation techniques propelled the adoption of LSF systems. Post-war, LSF walls surged in popularity, particularly in regions like North America, Australia, and [1] [2]

as architects and engineers recognized their numerous advantages including lightweight construction, expedited installation, design flexibility, and recyclability.

The first application of LSF systems extends back to the mid-19th century when both the United States and Britain initiated experiments with cold-formed steel applications around 1850 [3]. However, it wasn't until the 1940s that specific North American regulations for LSF construction began to solidify, paving the way for the widespread adoption of lightweight steel framing techniques seen today[1]. Over time, LSF systems continued to evolve, propelled by their inherent benefits such as high structural resilience, cost efficiency through rapid prefabrication, and sustainability due to recyclability and reusability.

1.3- LSF partition walls most recent fire event

On 22 February 2024, at approximately 17:30 CET, a fire broke out in a 14-storey residential complex located in the city of Valencia, Spain[4]. The rapid spread of the fire, exacerbated by strong winds, building materials and a stack effect, led to the complete destruction of the building 138 apartments, trapping numerous residents inside. Ten bodies were recovered from the building following an inspection by forensic police, and 15 people were injured during the blaze, including several firefighters. It is believed that immediately after the fire broke out in a 7th-floor apartment at around 17:30 CET, many lives were saved by the actions of one of the building's concierges (doormen) who banged on the residents' doors and ordered them to evacuate the building. Multiple witnesses nearby captured the early stages of the blaze on their smartphones, showing how it quickly intensified and began spreading across the façade and from the inside, see Figure 1. The protection layers are still visible, but most of them fall off during this event, losing the compartmentation effect.

Figure 1:View of the LSF walls exposed to fire. Photo captured by Monica Torres and published in “El Pais”[4].

Firefighters, ambulances and law enforcement arrived at the scene soon after. Witnesses indicated that the blaze had engulfed the entire first building “in a matter of 10 minutes”, and soon spread to the second. Due to the high temperatures, firefighters were only able to access up to the 12^{th} floor of the building but were able to rescue some residents. Winds of around 60 km/h were also recorded in the area at the time. Due to the strong wind, the fire was fanned and next to that the water jets were blown away from the building.

1.4- Plane of thesis

The second chapter provides an overview of the current state of the art, offering a retrospective analysis of studies concerning the fire resistance of LSF structures.

The third chapter defines the fire scenarios that can be used to analyse the fire insulation behaviour of the LSF walls. This chapter also presents the heat release rate during the freee burn of the materials.

The fourth chapter presents the main heat transfer modes and the requirements of the LSF wall under fire. The testing standards are also presented.

The fifth chapter presents the description of all wall specimens and thermocouple positions.

The sixth chapter presents the numerical model and the boundary conditions. This chapter also presents the importance of the bulk temperature of the cavity region. Some explanations of how the Finite Element Method (FEM) works in ANSYS are also presented.

The seventh chapter presents the numerical validation, using seven experimental results. This validation includes calculating the Root Mean Square Error and Relative Error for each specimen tested.

The eighth chapter presents the main conclusions of this investigation.

Chapter 2

2- STATE OF ART

LSF walls are walls that are made of light steel framing, which is a construction system that uses cold-formed steel sections as the main structural components. LSF walls can be either load-bearing or non-load bearing, depending on whether they support any vertical loads other than their own weight. LSF walls have many advantages, such as light weight, fast erection, design flexibility, and recyclability. The American Iron and Steel Institute (AISI) published the initial recommendations for design in 1946 [1]. In 1963, Prof. G. Winter conducted a considerable study at Cornell University on cold-formed steel components, analysing the impact of cold-straining on structural sheets [5].

The American Iron and Steel Institute paid for a Cornell University research study to determine how cold-forming affects mechanical behaviour [6]. In 1961, the British steel standard was updated to incorporate the design of cold formed steel members based on Prof. A. H. Chilver's findings [7]. The Australian standard for designing cold-formed steel structural elements was originally published in 1974[2]. This standard was based on the 1968 American standards, but with revisions to match beam and column design curves with the Australian Steel Structures Code. In 1994, the finite difference numerical model was presented by Mehaffey and Cuerrier et al [8]to perform studies across heat transfer in surfaces, and between surfaces and cavities. The model was validated with experimental tests.

Similar numerical methods are used in this work, applied to the calculations of heat transfer, being those calculations performed by the software ANSYS Multiphysics. This model is a 2D heat transfer model without fluid interaction, that uses partial differential equations to approach the results, using iterative and incremental procedures.

Other experimental investigations have been developed to analyze the effect of the fire protection material, the effect of the material grade, and the effect of the LSF type, such as: Y.

Sakumoto et al. in 2003 [9], Prakash Kolarkar in 2010 [10], Gunalan et al. in 2013 [11], Ayman Y. Nassif et al. in 2014 [12], S. Kesawan and M. Mahendran in 2015 [13], Anthony Deloge Ariyanayagam, Mahen Mahendran in 2017 [14]. More recently, Dias et al. [15] opted to investigate the behaviour of LSF walls using steel sheets. This sheeting is responsible for increasing the shear resistance at room temperature, but generated only moderate improvements in the stud temperature development.

The results in slight increases in load-bearing fire resistance. Magarabooshanam et al. [16] conducted an experiment in 2020 to study the effects of cavity depth on non-load bearing LSF walls, concluding that as cavity depth increases, temperatures throughout the wall depth fall, resulting in an increase in the assembly's insulation fire resistance. Tao et al. [17] also examined the impact of silica aerogel fiberglass blanket, when employed as an extra layer in contact with the LSF.

This substance enhances fire resistance, slowing the increase in stud temperature by 20 minutes. The primary disadvantage of this material is that it overheats the most exposed gypsum layers, resulting in board collapse. Gnanachelvam et al. [18] investigated different insulation materials and placements concerning the fire resistance of LSF walls. Externally insulated LSF walls have always had better insulation and fire resistance than cavity insulated LSF walls. Higher Hot Flange (HF) temperatures have been observed when the insulating material is positioned in the cavity region. The usage of cellulose with microencapsulated paraffin PCM did not decrease fire resistance and seemed to postpone failure.

However, this insulating material generated intense flames and thick smoke. PCM combined with cellulose may be advised for usage externally as a composite layer solution with gypsum in LSF wall systems to improve fire resistance and energy efficiency. Pancheti et al. [19] studied the fire resistance of load-bearing external walls with corrugated steel cladding, facing the exterior with ISO834. Corrugated steel cladding considerably increased LSF walls' load-bearing fire protection. The use of insulating material on the exterior side improves load bearing fire resistance as compared to the cavity location.

The results were compared to typical LSF walls without cavity insulation material and rockwool cavity insulation in both fire scenarios (ISO834 and hydrocarbon). For all fire scenarios, the insulation's fire resistance increased when the cavity was filled with rockwool and significantly when concrete foam was added. The use of rockwool in the cavity region reduced the ability to support the load under fire, but the application of lightweight concrete in the cavity enhanced

it, both in contrast to the LSF without insulating material in the cavity. The ability to support the load was determined utilizing a correlation between the load level and the critical temperature. The downside of filling the space with lightweight concrete is an increase in total weight.

Perera et al. [20] conducted a numerical analysis of the insulation and fire resistance of novel building walls. The use of back blocking in both stud flanges and discontinuous cavity insulation improves insulation fire resistance. When compared to empty and completely insulated (100%) solutions, using a 40% insulation ratio in the cavity is the most effective way to achieve enough fire resistance time for insulation and load carrying. The authors also created empirical models for calculating the load-bearing fire resistance of conventional and modular LSF walls with single layer and double layer sheathings.

Gardner et al[21] conducted a significant study on a novel hypothesis for the constitutive law of cold-formed steels. LSF walls with single layer and double layer sheathings

This research was based on over 700 experimental tests conducted throughout the world on a variety of steel grades, allowing the authors to offer an approximation based on the two-stage Ramberg-Osgood model. Two years later, Rokilan and Mahendran[22] proposed a novel model for this material's behaviour at increased temperatures, based on a two-stage Ramberg-Osgood model. New estimates for the reduction factors are offered, taking into account both High Strength Steel (HSS) and Low Strength Steel. New prediction equations for ultimate strength, stress at 2% total strain, 0.05% proof stress, and proportional limit stress have also been suggested.

The Polytechnic Institute of Bragança (Portugal) is also investigating the fire performance on LSF walls with the aim of: developing accurate numerical models based on thermal analysis with fluid-structure interaction [23], validating the numerical models with experimental tests developed elsewhere [24], analyzing the fire performance of LSF using the simplified one-dimensional heat flow [25], and presenting a sequential numerical model to study the fire resistance. This study also featured an original simplified procedure, and the findings were compatible with the experimental findings.

All of these experimental tests were carried out on reduced-scale LSF wall specimens. This publication offers a numerical model that has been thermally validated against reduced scale specimens and thermomechanically validated against full size specimens.

Because of the presence of several failure modes, these correlations vary with LSF size (reduced and full scale)Numerical studies were employed to validate the models and eliminate costly testing procedures. These simulations are also utilized for parametric studies, which determine the influence of design factors. In 1996, Mohamed Sultan [26] published the findings of the one-dimensional finite difference approach created to solve the heat transfer model and compared them to experimental data over time.

The model accounts for convection and radiation from both gypsum layers facing the hollow region, but ignores heat radiation from the steel studs to the gypsum surface. According to this source, the steel stud's influence on heat transfer through the gypsum layers is minor. This absence may explain the discrepancy between experimental data and model predictions. In comparison to the experimental data, this model provides conservative fire ratings. This study also describes the thermophysical characteristics of gypsum type X (hence referred to as Gypsum 2).

In 2002, Geoff Thomas [27] investigated the influence of thermal characteristics on gypsum plasterboard at extreme temperatures, developing a finite element thermal model for LTF walls. Thermal characteristics were altered to simulate physical processes like ablation and cracking, as well as to minimize numerical instabilities. In comparison to experimental measurements, the model was more cautious and less accurate. Thermal characteristics were judged effective and thought to be appropriate for use in finite element models. In 2004 [28], C. Ang and Y. Wang examined the influence of moisture flow in gypsum layers using heat and mass transfer.

The authors opted to use an equivalent (effective) specific heat, greater than the latent heat of water evaporation to skip the mass analysis and utilize it simply in the thermal analysis, without addressing explicitly the moisture movement. Keerthan P. and Mahendran M. in 2012 [29] examined the fire performance of numerous layers of gypsum boards (without simulating the LSF system) using the SAFIR program and some earlier practical tests to confirm the results.

This study used reduced-scale specimens to investigate thermal performance under fire with various gypsum thermal characteristics. This study emphasizes the danger of stepping over the evaporation process from the gypsum substance. To avoid this danger, these authors adopted a material attribute specified by the enthalpy equation.

Chapter 3

3- FIRE SCENARIOS

“Fire scenarios” refer to planned or hypothetical situations that involve fires, encompassing a range of contexts and applications. These scenarios are often used for emergency preparedness, fire safety training, risk assessment, fire investigation, and firefighting tactics. They help individuals and organizations understand the causes, behavior, and consequences of fires, as well as develop effective strategies for prevention, mitigation, and response. Through the analysis of various fire scenarios, individuals can enhance their preparedness, safety awareness, and ability to respond to fire emergencies efficiently and effectively.

3.1- Localized fires

Localized fires are specific incidents where fire occurs within a relatively restricted area, as opposed to larger-scale wildfires or conflagrations. These fires can occur indoors or outdoors and are often confined to a single structure, room, vehicle, or small area of vegetation.

Indoor localized fires may originate from sources such as kitchen accidents, electrical malfunctions, heating systems, or flammable materials. For instance, a cooking mishap could lead to a fire in the kitchen of a residence, while an electrical short circuit might cause a fire in an office building.

Outdoor localized fires can result from various causes, including discarded cigarettes, campfires, burning debris, or equipment malfunctions. These fires typically occur in urban or suburban environments, but they can also happen in natural areas like parks, forests, or grasslands.

The management of localized fires often involves prompt intervention by firefighting personnel or individuals equipped with fire extinguishers. The goal is to contain the fire before it spreads beyond its initial point of origin. Firefighters use techniques such as water or foam suppression, ventilation, and structural firefighting to extinguish the flames and prevent further damage.

3.2- Small fires

Small fires are characterized by their limited size and localized nature, making them distinct from larger and more widespread incidents. These fires typically encompass areas such as small sections of buildings, individual rooms, vehicles, or outdoor spaces. Despite their relatively contained scope, small fires can still pose risks to property, safety, and the environment if not promptly addressed.

Indoor small fires often occur in kitchens, where cooking activities involving grease, oil, or other flammable materials can lead to ignition. Electrical malfunctions, such as overloaded circuits or faulty appliances, are another common cause of indoor small fires in homes, offices, or commercial establishments. Additionally, small fires may result from incidents like candles left unattended, smoking materials, or heating equipment accidents.

Outdoor small fires may originate from activities like burning yard waste, disposal of hot ashes, or sparks from machinery or equipment. Campfires, barbecues, and outdoor cooking activities can also lead to small fires if not properly managed and extinguished.

Managing small fires typically involves swift action to contain and extinguish the flames before they escalate. Individuals may use portable fire extinguishers, water hoses, or other firefighting equipment to suppress the fire and prevent its spread. Quick response is crucial to prevent small fires from growing larger and causing more extensive damage or posing greater risks to safety.

3.3- Hydrocarbon fires

In the context of fire scenarios, communication regarding hydrocarbons involves understanding their properties, risks, and behaviours in the event of a fire. Here are some key points to consider when communicating about hydrocarbons in fire scenarios:

Hydrocarbons are highly flammable substances due to their chemical composition, which makes them prone to combustion when exposed to ignition sources such as sparks, flames, or heat.

It's essential to identify potential ignition sources that can trigger the combustion of hydrocarbons, including electrical sparks, hot surfaces, open flames, or mechanical friction.

When a fire involves hydrocarbons, it can exhibit rapid and intense burning due to the high energy content of these fuels. Jet fires, pool fires, and vapour cloud explosions are examples of fire scenarios involving hydrocarbons.

Hydrocarbon fires can release toxic gases, smoke, and heat, posing risks to human health, property, and the environment. Understanding the hazards associated with hydrocarbon fires is crucial for implementing safety measures and emergency response protocols.

3.4- External fires

External fires, such as wildfires or fires originating from adjacent buildings or vegetation, can significantly impact fire scenarios in various settings. In urban or suburban environments, external fires can pose a threat to buildings and infrastructure, leading to the potential spread of flames and heat transfer to neighbouring structures. Fire scenarios involving external fires often require consideration of factors such as fire exposure duration, intensity, and direction of fire spread.

External fires can influence evacuation strategies and emergency response plans. Fire scenarios may need to account for the potential impact of external fires on evacuation routes, access roads, and the availability of emergency services. Understanding the behaviour of external fires, including their rate of spread and potential for ember showers, is crucial for developing effective evacuation procedures and ensuring the safety of occupants.

The interaction between external fires and built environments can affect fire dynamics and the performance of fire protection systems. Fire scenarios involving external fires may require the assessment of building envelope integrity, the effectiveness of fire-resistant barriers, and the vulnerability of exterior cladding materials to radiant heat exposure. Designing buildings and

infrastructure to withstand external fire events is essential for enhancing resilience and minimizing the risk of fire-induced damage.

3.5- Heat release rate

The Heat Release Rate (HRR) is a fundamental parameter within the field of fire science and engineering, offering a quantitative measure of the rate at which heat energy is liberated by a fire. Expressed typically in units of kilowatts (kW) or megawatts (MW), the HRR serves as a crucial indicator of the intensity, dynamics, and hazards associated with fires of varying scales. This metric is instrumental in comprehending the behaviour of fires, aiding in the development of effective strategies for fire suppression, evacuation, and mitigation.

Several key factors intricately influence the Heat Release Rate of a fire. Firstly, the characteristics of the fuel being consumed play a pivotal role. Factors such as fuel type, quantity, and properties significantly impact the energy released during combustion. For instance, combustible materials like wood, plastics, and hydrocarbons exhibit diverse combustion behaviours, thereby producing distinct HRR profiles. Additionally, ventilation conditions exert a notable influence on the HRR. The availability and configuration of ventilation openings dictate the supply of air to the fire, thereby modulating the combustion process and subsequently affecting the rate of heat release. Effective ventilation management can either enhance or suppress the combustion process, leading to discernible changes in the fire's HRR.

Furthermore, the stage of fire growth and decay also plays a crucial role in determining the HRR. Fires typically progress through distinct stages, including ignition, growth, fully developed burning, and decay. Each stage is characterized by specific changes in the fire's heat release rate. For example, during the growth phase, the HRR tends to increase rapidly until it reaches a peak, signifying the maximum heat output of the fire. Subsequently, in the fully developed burning stage, the HRR remains relatively constant before gradually declining during the decay phase as the available fuel is consumed.

3.6- Effects in the compartment

The Heat Release Rate (HRR) of a fire plays a pivotal role in shaping the environment within a room or enclosed space during a fire incident. Its effects are multifaceted and profoundly influence various factors critical to fire safety and emergency response.

Firstly, the HRR directly impacts the temperature dynamics within the room. Fires with higher HRRs generate more intense heat, leading to faster temperature increases within the space. Elevated temperatures pose significant risks to occupants, as they can cause thermal injuries, impair respiratory function, and compromise the structural integrity of the building.

Moreover, the HRR has a pronounced effect on smoke production during a fire. Higher HRRs result in greater volumes of smoke being generated, which can quickly fill the room and reduce visibility to near zero. Thick smoke not only impedes occupants' ability to navigate and locate exits but also exacerbates respiratory hazards, increasing the likelihood of smoke inhalation injuries and fatalities.

In addition to smoke, fires with elevated HRRs release higher concentrations of toxic gases into the environment. Combustion of various materials emits hazardous gases such as carbon monoxide (CO), hydrogen cyanide (HCN), and volatile organic compounds (VOCs). These gases can have severe health consequences, including asphyxiation, poisoning, and long-term respiratory ailments.

3.7- Energy release rates based on free burning

The energy release rate based on free burning is a pivotal parameter within fire science and engineering, offering a quantifiable measure of the rate at which energy is liberated during the combustion of a fuel in an unconstrained or freely burning state. This metric, typically expressed in units of power per unit area such as kilowatts per square meter (kW/m^2) or megawatts per square meter (MW/m^2).The nature of materials used in the construction of a Light Steel Frame (LSF) wall significantly affects the energy released during a fire. Combustible materials, such as wood, certain types of insulation have higher heat release rates (HRR) compared to non-combustible materials like steel.

Combustible materials in LSF walls can cause a fire to develop more rapidly and release more energy than the ISO 834 fire curve predicts. Materials with high HRR contribute to faster temperature increases and higher peak temperatures, deviating from the standardized curve.

The ISO 834 fire curve does not account for variations in material combustibility, ventilation, and compartment geometry, which are critical factors in real fires.

Chapter 4

4- FIRE AND HEAT TRANSFER

This chapter discusses the thermal load during a fire and provides directions for doing computational and experimental studies on this topic. A fire requires the simultaneous presence of three factors: a heat source, fuel, and an oxidizing, beginning when the mixture of fuel and oxidizer is hot enough to ignite.

4.1- Mechanisms of Heat Transfer

Mechanisms of heat transfer involve three main processes: conduction, convection, and radiation. Here's a brief explanation of each along with their respective equations.

4.1.1- Conduction

Conduction is the transfer of heat through a material or between materials that are in direct contact. It occurs due to the collision of molecules within a substance, transferring thermal energy from hotter regions to colder ones. The rate of heat conduction (Q) through a material can be calculated using Fourier's law:

$$Q = -k \cdot A \cdot dx/dT \quad (1)$$

Q is the rate of heat transfer (W or J/s), k is the thermal conductivity of the material (W/(m·K)), A is the cross-sectional area perpendicular to the direction of heat transfer (m^2), and dT/dx is the temperature gradient (K/m).

4.1.2- Convection

Convection is the transfer of heat through a fluid (liquid or gas) by the movement of the fluid itself. This movement can be natural (natural convection) or forced (forced convection), such as by a fan or pump. The rate of convective heat transfer (Q) can be calculated using Newton's law of cooling.

$$Q = h \cdot A \cdot (Ts - T\infty) \quad (2)$$

Where Q is the rate of heat transfer (W or J/s), h is the convective heat transfer coefficient ($W/(m^2 \cdot K)$), A is the surface area over which convection occurs (m^2), Ts is the surface temperature (K), T∞ is the fluid temperature far from the surface (K).

4.1.3- Radiation

Radiation is the transfer of heat in the form of electromagnetic waves, without the need for a medium. All objects emit radiation, with the rate of emission depending on their temperature and emissivity. The Stefan-Boltzmann law describes the rate of radiative heat transfer from a surface.

$$Q = \varepsilon f . \varepsilon m \cdot \sigma \cdot A \cdot (Ts4 - T\infty 4) \quad (3)$$

Q is the rate of heat transfer (W or J/s), εf is the emissivity of the material (both dimensionless), σ is the Stefan-Boltzmann constant (5.67×10^{-8} $W/(m^2 \cdot K^4)$), A is the surface area emitting

radiation (m^2), Ts is the surface temperature of the material (K), and $T\infty$ is the temperature of the surroundings (K).

These equations are fundamental in understanding and analysing heat transfer in various systems and scenarios.

4.2- Direction of Heat Flow

In an LSF (Light Steel Framing) wall, the direction of heat flow depends on several factors, including the thermal conductivity of the materials involved, the temperature difference across the wall, and the presence of insulation.

The direction of heat flow is always from a region of higher temperature to a region of lower temperature. This fundamental principle is known as the second law of thermodynamics. Heat naturally moves from areas of high thermal energy to areas of lower thermal energy until thermal equilibrium is reached, meaning that the temperatures become equalised.

This directional movement ensures that thermal energy is distributed evenly throughout a system, and it drives many natural processes such as conduction, convection, and radiation. Understanding the direction of heat flow is essential in various fields including engineering, physics, and environmental science, as it allows for the prediction and control of temperature distributions in systems and environments.

4.3- Fire Performance of LSF Walls

LSF walls, constructed from cold-formed steel frames and fire-resistant gypsum plasterboards, serve as integral components in modern building construction. These walls, whether load-bearing or non-load bearing, are essential for ensuring structural integrity and safety in both residential and commercial structures. Traditionally, fire design methods for LSF walls have leaned heavily on prescriptive approaches, leveraging fire resistance ratings (FRR) supplied by manufacturers. However, emerging research endeavours have shed light on numerous factors that significantly influence the fire performance of LSF walls. These factors include the composition and arrangement of materials, the presence of insulation, the configuration of wall

assemblies, and the overall design considerations. By delving into these complexities, recent studies aim to enhance our understanding of LSF wall behaviour in fire scenarios, paving the way for more robust and reliable fire protection strategies. Through a deeper exploration of these parameters, designers and engineers can refine fire design methodologies and develop innovative solutions to bolster the fire resilience of LSF wall systems, ultimately advancing the safety and durability of modern construction practices.

4-4- Parameters Influencing Fire Performance

Several parameters play crucial roles in influencing the fire performance of LSF (Light Steel Framing) walls. Understanding these factors is essential for designing and constructing buildings with enhanced fire resilience. The following sections present some key parameters.

4.4.1- Material Composition

The materials used in constructing LSF walls significantly impact their fire performance. Cold-formed steel frames are commonly used due to their strength and durability. Fire-resistant gypsum plasterboards are often used as lining materials to provide a protective barrier against fire. The type and quality of these materials can affect how well the wall withstands fire exposure.

4.4.2- Insulation

Insulation materials incorporated within the wall assembly can affect its fire performance. Insulation helps regulate heat transfer and can delay the spread of fire. Different types of insulation, such as mineral wool or foam boards, have varying fire-resistant properties and can help to increase the LSF wall performance. The thickness and placement of insulation layers also influence heat transfer through the wall assembly.

4.4.3- Wall Configuration

The configuration of LSF walls, including the arrangement of framing members, plasterboard lining, and insulation layers, can impact their fire resistance. For example, double-layer plasterboard linings or the use of fire-resistant coatings on steel members can enhance fire performance.

4.4.4- Cavity Size and Design

The size and design of cavities within LSF walls can affect fire performance. Larger cavities may allow for slower heat transfer, while well-designed cavities with appropriate insulation can improve fire resistance. The presence of voids or gaps in the wall assembly can also affect the spread of fire.

4.4.5- Load Bearing Capacity

In load-bearing LSF walls, the structural integrity of the framing members under fire conditions is critical. The load-bearing capacity of steel studs and connections can influence the wall's ability to withstand fire-induced loads without collapsing. The higher the load level the smaller the fire resistance time and also the smaller the critical temperature[STRUCTURAL DESIGN FOR FIRE SAFETY Second Edition Andrew H. Buchanan & Anthony K. Abu University of Canterbury, New Zealand].

4.4.6- External Factors

External factors such as building orientation, surrounding fire hazards, and proximity to other structures can influence the fire performance of LSF walls. Wind patterns, ambient temperature,

and exposure to direct flames or radiant heat from adjacent fires can all impact the severity of fire exposure.

4.5- Fire Resistance Testing Standards

Fire resistance testing standards provide rules and processes for determining the capacity of building materials and components to survive fire. These criteria are critical to ensure the safety and longevity of structures, particularly LSF (Light Steel Framing) walls. Here are several widely accepted fire resistance testing standards:

ISO834 [30] (Furnace temperature- Heating curve);

EN 1363-1 [31] (criteria for insulation - tolerance);

EN 1364-1 [32] (test partition walls ‘position thermocouples’);

EN 13501-2 [33] (The design of the test specimen);

EN 1991-1-2 [34] (Thermal actions for temperature analysis).

4.5.1- Standard ISO 834

ISO 834, published by the International Organization for Standardization (ISO), delineates fire resistance testing procedures for building elements, but is not updated since 1999. It plays a critical role in ensuring safety and compliance with legal obligations regarding fire prevention and life safety in buildings. ISO 834 defines fire exposure conditions, such as temperature-time curves, as crucial for evaluating the fire resistance of structural components.

where the fire load burns over a specific period causing temperatures to eventually drop, the ISO standard fire curve maintains a constant increase in temperature. Natural fires are influenced by various factors such as the availability of oxygen and the thermal properties of the building’s structure (including walls, roof, and floor), which makes their behaviour more unpredictable and irregular. Consequently, the ISO standard fire curve is considered artificial because it does not account for these fluctuations and conditions that affect a real fire's progression.

The average temperature of the furnace, as derived from the thermocouples, shall be monitored and controlled such that it follows the relationship:

$$T = 20 + 345\, log_{10}(8t + 1) \quad (4)$$

where T is the average furnace temperature, in degrees Celsius and t is the time, in minutes, see Figure 2.

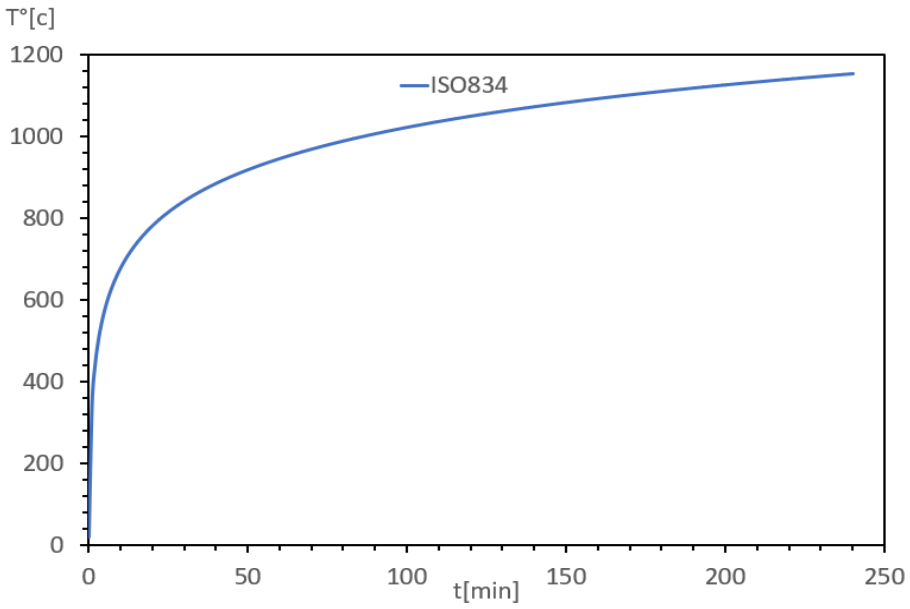

Figure 2: Standard time/temperature curve.

4.5.2- Standard EN 1363-1

The performance criteria used to validate the tests of fire resistance of non-load bearing walls are the insulation criteria (I). By definition this is the time, in completed minutes, for which the test specimen continues to maintain its separating function during the test without developing temperatures on its unexposed surface, which increases the average temperature above the initial average temperature by more than 140 K or increase at any location (including the roving thermocouple) above the initial average temperature by more than 180 K. The performance criteria "insulation" shall automatically be assumed not to be satisfied when the "integrity" criterion ceases to be satisfied. The integrity criteria (E), in this case, concerns about the time of flame or smoke passing through the unexposed side by some crack.

One of the critical aspects addressed in EN 1363-1 is the tolerance in temperature measurements during the test. Accurate temperature control is essential to ensure the validity and reproducibility of the fire resistance tests. After the initial 10 minutes of the test, the temperature measured by any thermocouple within the furnace must not deviate from the standard temperature/time curve by more than 100 K. However, if the test specimen burns quickly, causing a sudden ignition of significant amounts of combustible material, a temperature deviation greater than 100 K above the specified curve is permissible for a maximum of 10 minutes. This excess deviation must be clearly identified as resulting from the rapid ignition of these materials, which increases the furnace's gas temperature.

4.5.3- Standard EN1364-1

EN 1364-1 is a European standard that specifies methods for determining the fire resistance of non-loadbearing walls. In this test, thermocouples are positioned at specific locations to measure temperatures during the fire exposure. The positioning of thermocouples is critical for accurately assessing the performance of partition walls under fire conditions.

According to EN 1364-1, thermocouples are typically placed at various locations within the test specimen, including the surface thermcouples. These are positioned on the exposed surfaces of the partition wall to measure the temperature rise during the fire test. Surface thermocouples are placed at different heights and distances from the fire source to capture temperature variations across the wall surface. Other important thermocouples are the internal. These are inserted into the core or cavity of the partition wall to monitor temperature changes within the structure. Internal thermocouples provide insights into heat penetration and the integrity of insulation materials during the fire exposure. There are also thermocouples used for the critical locations. These thermocouples may also be placed at critical locations identified based on the design and construction of the partition wall. These locations include areas prone to failure or where structural components are vulnerable to fire damage.

4.5.4- Standard EN13501-2

The design of the test specimen and the number of tests to be carried out shall be derived from a comparison between the envisaged field of application of the classification and the field of application of test results as defined in the test standard. Every test method provides information on the following: test specimen; field of direct application of test results; and guidance on test specimen design especially for testing glazed elements or non-loadbearing walls incorporating glazings.

The assessment of integrity (E) shall be made based on the following three aspects:

a) cracks or openings in excess of given dimensions;

b) ignition of a cotton pad;

c) sustained flaming on the non-exposed side.

Classification of integrity (E) shall be according to whether or not the element is also classified for insulation (I). Where an element is classified both for integrity (E) and thermal insulation (I), the integrity value shall be determined by whichever of the three criteria fails first. Where an element is classified (E) but without an (I) classification, the integrity value shall be defined as the time to failure of only the cracks/openings or sustained flaming criteria, whichever fails first.

The performance level, used to define thermal insulation, shall be the mean temperature rise on the unexposed face, limited to 140 °C above the initial average temperature, or with the maximum temperature rise at any point limited to 180 °C above the initial average temperature. The test standard specifies how both for uniform and non-uniform elements the mean temperature shall be determined. For an element incorporating discrete areas of different thermal insulation, compliance with the thermal insulation criteria shall be determined separately for each area.

The classification for partition walls is defined in Europe according to Table 1.

Table 1: Fire ratings for partition walls.

E		20	30		60	90	120		
EI	15	20	30	45	60	90	120	180	240
EI-M			30		60	90	120	180	240
EW		20	30		60	90	120		

Table 2 that introduces the fire ratings for partition walls, including de definition of **E**, **EI**, **EI-M**, and **EW**.

Table 2: Description and definition of the fire ratings for partition walls.

Rating	**Description**	**Definition**
E	Integrity	The ability to prevent flames and hot gases from passing through.
EI	Integrity and Insulation	The ability to maintain structural integrity and provide thermal insulation during a fire.
EI-M	Integrity, Insulation, and Mechanical Load	The ability to withstand fire exposure while supporting the designed load.
EW	Integrity and Radiation	The ability to prevent the passage of flames and limit the transfer of thermal radiation.

4.5.5- Standard EN 1991-1-2

EN 1991-1-2 is a European standard that deals with the actions on structures exposed to fire. In section 3, it discusses the various types of actions or loads that structures may be subjected to during a fire event. This could include factors such as thermal effects, mechanical effects, and the behavior of materials under high temperatures.

For surfaces exposed to fire, hnet is calculated by combining convection and radiation heat transfers:

$$h_{net} = h_{net,c} + h_{net,r}\ [W/m^2] \quad (5)$$

Where:

$$h_{net,c} = \alpha_c \cdot (\Theta g - \Theta m)\ [W/m^2] \quad (6)$$

where α_c is the convection heat transfer coefficient [W/m²K], Θg is the gas temperature near the fire-exposed member [°C], and Θm is the member's surface temperature [°C]. For the coefficient of heat transfer by convection α_c, the relevant value should be selected, depending on the temperature-time curves.

- Standard temperature-time curve (ISO834) : αc = 25 [W/m^2 K].
- External fire curve: αc = 25 [W/m^2 K].
- Hydrocarbon curve: αc = 50 [W/m^2 K].
- Natural fire models: αc = 35 [W/m^2 K].

For the unexposed side, h_{net} is calculated using an equation with α_c=4 [W/m²K]. When accounting for radiation effects, α_c is taken as 9 [W/m²K].

$$h_{net,r} = \Phi \cdot \epsilon m \cdot \epsilon f \cdot \sigma \cdot [(\Theta r + 273.15)^4 - (\Theta m + 273.15)^4]\ [W/m^2] \quad (7)$$

where Φ is the view factor, ϵm is the member's surface emissivity, ϵf is the flame emissivity, σ is the Stefan-Boltzmann constant (5.67 × 10^{-8} W/m²K⁴), Θr is the effective radiation temperature of the fire environment [°C], and Θm is the member's surface temperature [°C].

Chapter 5

5- WALL SPECIMENS

The tracks used are U93x43x1.5 for specimens (3,4,5,6and7) and U92x40x0,95 for specimens (1and2), steel grade S280GD, and the studs are C90x43x15x1,5 for specimens (3,4,5,6and7) and C90x36x7x0,75for specimens(1and2), steel grade S280GD. Five, four and three studs per track were adopted to investigate the effects of the different materials for plates in the structure. The material configuration for the walls was: single gypsum plasterboard, double gypsum plasterboard, cork-gypsum plasterboard composite and cellulose-gypsum plasterboard composite. For the cork, a special study will be conducted, keeping the cork-gypsum plasterboard composite and modifying the number of the studs, this constructive solution was selected to evaluate the fire performance. A test with rock wool was also conducted, to evaluate the fire performance of the insulation material inside the cavity.

The Table 3 shows the specimens to be tested and their configurations.

Table 3:The specimens to be tested and their configurations.

SPECIMEN ID	NUMBER OF STUDS	SPACING STUDS [mm]	TYPES OF STEEL SECTIONS	MATERIAL / THICKNESS [mm] LAYER 1	MATERIAL / THICKNESS [mm] LAYER 2	MATERIAL / THICKNESS [mm] LAYER 3	CAVITY /DENSITY [kg/m^3] INSULATION
1	3	450	C90x36x7x0,75/ S280GD(studs) U92x40x0,95/ S280GD (tracks)	Gypsum/16	Gypsum/16	-	Cellulose/50
2	3	450	C90x36x7x0,75/ S280GD(studs) U92x40x0,95/ S280GD (tracks)	Gypsum/16	Cellulose/10	Gypsum/16	-
3	5	233	C90x43x15x1,5/ S280GD(studs) U93x43x1.5 S280GD (tracks)	Gypsum/ 12,5	-	-	Rockwool/75
4	5	233	C90x43x15x1,5/ S280GD(studs) U93x43x1.5 S280GD (tracks)	Gypsum/12,5	-	-	-
5	3	466	C90x43x15x1,5/ S280GD(studs) U93x43x1.5 S280GD (tracks)	Gypsum / 12,5	Cork/10	-	-
6	4	487.5	C90x43x15x1,5/ S280GD(studs) U93x43x1.5 S280GD (tracks)	Gypsum / 12,5	Cork/10	-	-
7	4	487,5	C90x43x15x1,5/ S280GD(studs) U93x43x1.5 S280GD (tracks)	Gypsum / 12,5	-	-	-

5.1- Description of specimens and the temperature control point positions

This chapter presents the description of each specimen and the temperature control point positions.

5.1.1- The specimen 1

Figure 3 shows the location of the temperature control point for test specimen 1, which was made of double layers of gypsum plasterboards lined on both sides of the studs with cellulose insulation in the cavity.

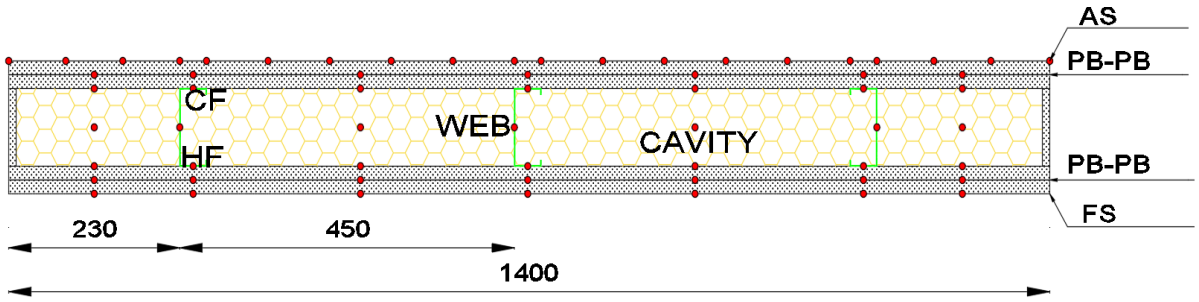

Figure 3: The location of the temperature control point for test specimen 1.

5.1.2- The specimen 2

Figure 4 shows the location of the temperature control of the test specimen 2, made of double layers of gypsum plasterboards on both sides of the studs and filled with external cellulose insulation sandwiched between the two plasterboard layers Figure 5.

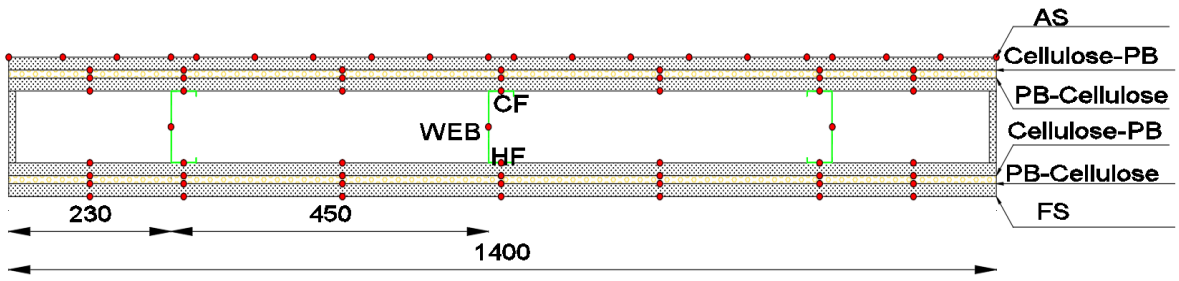

Figure 4: The location of the temperature control point for test specimen 2.

5.1.3- The specimen 3

Specimen 3 consists of a single layer of plasterboard with the cavity filled with Rockwool insulation. The Rockwool used has a density of 75 kg/m³. Temperature control points are strategically placed within the specimen, as illustrated in Figure 5, to measure the temperature within the insulation material.

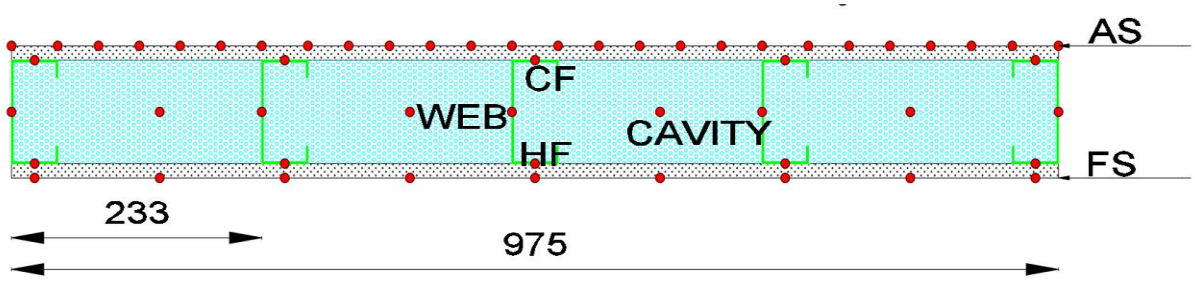

Figure 5: The location of the temperature control point for test specimen 3.

5.1.4- The specimen 4

The specimen 4 has the same LSF structure of the specimen 3, but without insulation in the cavity. Temperature control points used in this test are presented in the Figure 6.

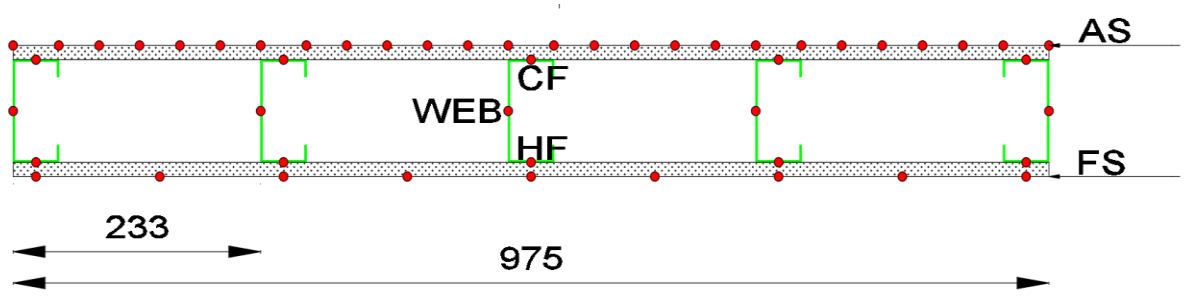

Figure 6: The location of the temperature control point for test specimen 4.

5.1.5- The specimen 5

The specimen 5 has 3 studs. That solution creates two cavities in both directions, bigger than the dimensions of the cavities in LSF structure with 5 studs. made of a layer of gypsum plasterboards and a layer of cork with a density of 50 kg/m3, applied on both sides of the specimen. Temperature control points used in this test are presented in the Figure 7.

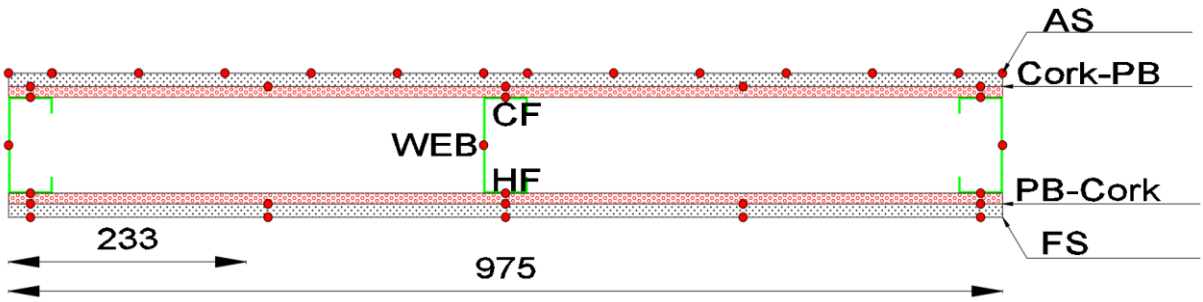

Figure 7: The location of the temperature control point for test specimen 5..

5.1.6- The specimen 6

The specimen 6 is the second specimen with a composite layer of cork and gypsum. This LSF wall has 4 studs producing 2 cavities. Temperature control points are presented in the Figure 8.

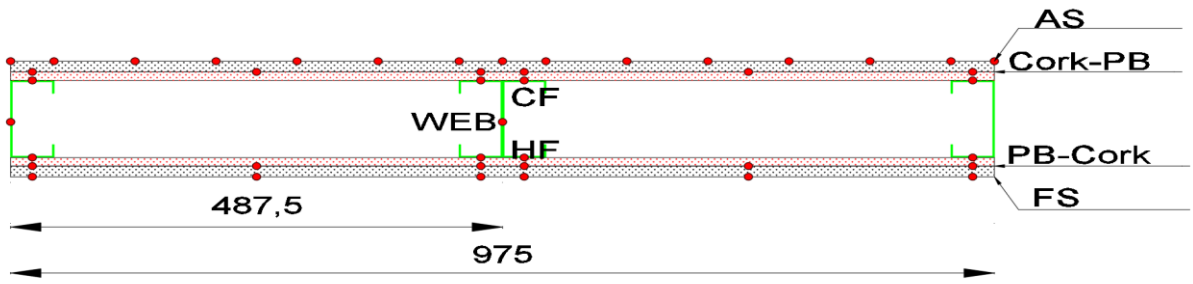

Figure 8: The location of the temperature control point for test specimen 6.

5.1.7- The specimen 7

The specimen 7 has the same number of studs as specimen 6 without the presence of cork layer. Temperature control points are presented in the Figure 9.

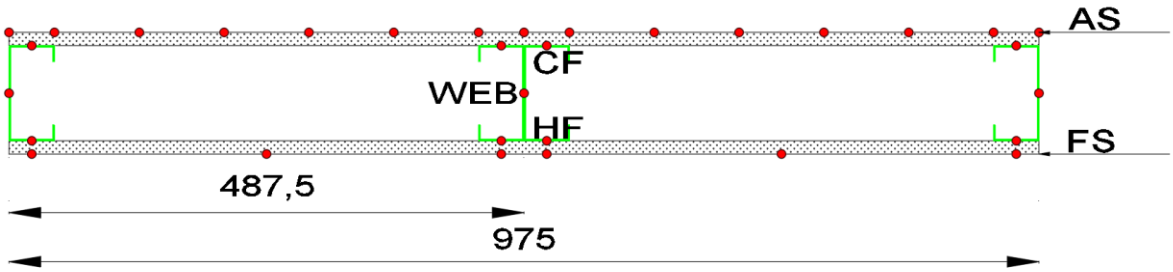

Figure 9: The location of the temperature control point for test specimen 7.

Chapter 6

6- NUMERICAL MODEL

This chapter presents the boundary conditions, the importance of the bulk temperature, and some explanations of how The Finite Element Method (FEM) works in ANSYS.

6.1- Boundary Conditions

The boundary criteria are based on EN1991-1-2. One side of the wall is exposed to fire, while the other is exposed to ambient temperature. To account for the radiation, heat flux by radiation (emissivity of fire εf = 1) and convection (convection coefficient α = 25W/m^2°C) on the fire side is assumed, and heat flux by convection (convection coefficient α = 9W/m^2°C) on the unexposed side is assumed to include the radiation effect.

The gas temperature on the fire side follows the ISO834 standard. Throughout the simulation, the gas in contact with the unexposed surface remains with constant temperature and equal to the initial temperature, usually T = 20 °C, see Figure 10.

To validate the numerical model, several simulations were developed to calculate the temperature field in the walls, with fire resistance defined by the temperature evolution on the unexposed side. The solution approaches and models were validated using experiments developed by Prakash Kolarkar [10].

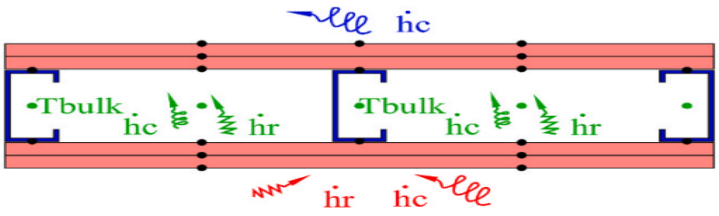

Figure 10: Boundary Condition for void cavities using the hybrid method. [31].

6.2- Importance of Bulk temperature

The bulk temperature may be given as an average of the hot and cold flanges and is intended to reflect any damage during the test. A Bulk temperature value was taken from the experimental test of the hot and cold flanges and introduced in Ansys as an extra boundary condition, considering the radiation and convection heat transfer, see Figure 10. This is called the hybrid method. Table 4 presents an example of the bulk temperature used for specimen 4. This temperature evolution was determined by the average between the Hot Flange (HF) and the Cold Flange (CF).

Table 4: The bulk temperature the hot and cold flanges temperature used for specimen 4.

Time (min)	**Time (s)**	**HF (ºC)**	**CF (ºC)**	**Bulk (ºC)**
0	0	21,59	21,59	21,59
10	600	95,13	84,33	89,73
20	1200	168,67	105,70	137,18
30	1800	351,95	209,82	280,89
40	2400	411,10	290,56	350,83
50	3000	459,45	355,10	407,27
60	3600	511,40	417,84	464,62
70	4200	561,54	487,78	524,66
80	4800	604,52	537,95	571,24

Figure 11 presents the bulk temperature, the hot and cold flanges temperature used for specimen 4.

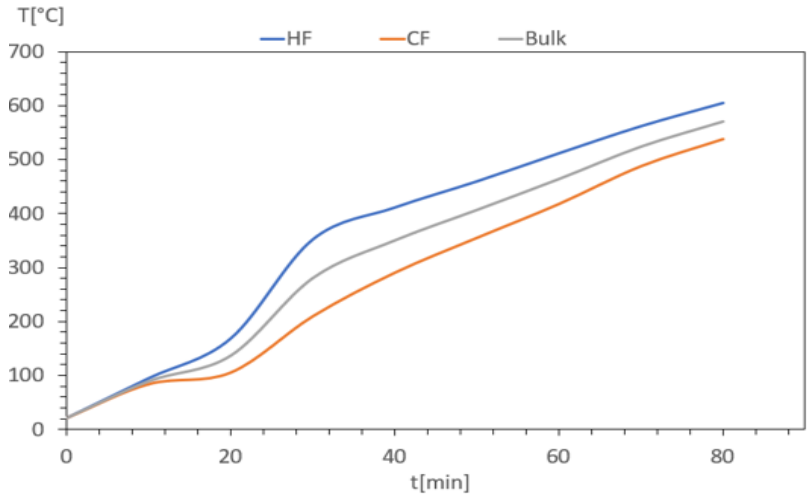

Figure 11: The bulk temperature the hot and cold flanges temperature.

6.3- The finite element method

The Finite Element Method (FEM) in ANSYS software is a computational technique used to analyse the behaviour of complex structures and systems under various conditions, including thermal, structural, fluid flow, and electromagnetic effects. Here's an explanation of how FEM works in ANSYS.

6.3.1- Mesh Generation

FEM begins with the creation of a mesh, where the geometry of the structure is discretized into small, interconnected elements. This process divides the structure into manageable elements for analysis. ANSYS provides tools to generate structured or unstructured meshes, depending on the geometry and requirements of the analysis.

6.3.2- Solution

ANSYS solves the system of equations using numerical methods, such as matrix inversion or iterative techniques, to determine the response of the structure. This includes computing

temperature distributions, stress and strain fields, fluid velocities, or electromagnetic fields, depending on the type of analysis being performed. This solution method is incremental in time and iterative. The convergence criterion is defined based on the heat flow.

6.3.3- Iterative Procedure

FEM in ANSYS often involves an iterative process, where user can refine the mesh, adjust boundary conditions, or modify material properties to improve the accuracy of the analysis results.

Finite Element Methods in ANSYS software provide users with powerful capabilities for simulating and analyzing the behaviour of complex systems, including LSF walls, under various thermal conditions. These simulations help users to optimize designs, evaluate performance, and ensure compliance with safety and regulatory standards.

Iterations are also included, whenever the material properties are temperature-dependent. This requires a convergence criterion to stop this process.

6.3.4- Element types used in the specimens

Plane 55, Link 31, and Link 34 are different element types available in ANSYS software, each tailored for specific types of thermal analysis. Plane 55 is used for plane solid surfaces, Link 31 is used for heat flow radiation over the cavity region, and Link 34 is used for heat flow by convection over the cavity region. Choosing the appropriate element type depends on the geometry, loading conditions, and desired level of accuracy in the analysis.

In ANSYS software, "Plane 55" refers to a specific element type used in finite element analysis (FEA). Similarly, "Link 31" and "Link 34" refer to other element types. Here's a brief explanation of each.

6.3.4.1- Plane 55 Element

"Plane 55" refers to a specific element type used primarily for thermal analysis. Plane 55 is a 2D thermal element utilised to model temperature distribution and heat conduction in a two-dimensional plane.

Plane 55 is a two-dimensional, four-node thermal element. Each node has a single degree of freedom: temperature. The element is defined by four nodes in a quadrilateral shape. The element can also be degenerated into a triangular shape if necessary (avoid).

The element is able to be used in transient thermal analysis. Suitable for modelling heat conduction in solids. See the Figure 12

The shape functions and or interpolating functions, Ni, for a four-node quadrilateral element in terms of natural coordinates (ξ, η) are:

$$\begin{aligned} N1&=\frac{1}{4}(1-\xi)(1-\eta) \\ N2&=\frac{1}{4}(1+\xi)(1-\eta) \\ N3&=\frac{1}{4}(1+\xi)(1+\eta) \\ N4&=\frac{1}{4}(1-\xi)(1+\eta) \end{aligned} \tag{8}$$

The temperature field T_i within the element can be expressed as:

$$T(\xi,\eta)=N1xT1+N2xT2+N3xT3+N4xT4 \tag{9}$$

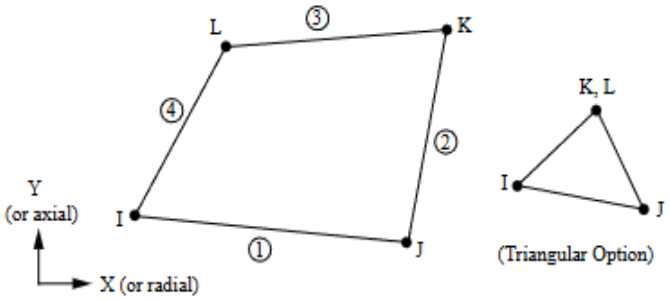

Figure 12: Plane55 [37].

6.3.4.2- Link 31 Element

Link 31 is a uniaxial element which models the radiation heat flow rate between two points in space. The link has a single degree of freedom, temperature, at each node. The radiation element is applicable to 2-D scenarios (plane or axisymmetric) and 3-D scenarios. It accommodates both steady-state and transient thermal analysis. This element does not use any interpolating function or any numerical integration method. The area of the heat flow is to be defined, the resultant emissivity is required and the view factor. See the Figure 13

Figure 13: Link31[37]

6.3.4.3- Link 34 Element

Link 34 is a one-dimensional, like Link 31 This element type possesses the capability to convection heat between its nodes. This element type Similar to Link 31. Link 34 also has temperature as its single degree of freedom at each node. Link 34 is suitable for 2-D (plane or axisymmetric) and 3-D scenarios and it Supports both steady-state and transient thermal

analysis. This element requires the definition of the area for the heat flow, the convection coefficient, and eventually the empirical coefficient. See the Figure 14

Figure 14: Link34[37]

6.3.5- The materials properties

Thermal properties refer to the characteristics of a material that determine its behaviour in response to changes in temperature. These properties play a crucial role in various engineering applications, particularly in heat transfer analysis and material selection for thermal insulation or conductivity. Some of the most important thermal properties include the thermal conductivity, the specific heat, density and emissivity.

6.3.5.1- Thermal Conductivity

Thermal conductivity is a physical property of a material that measures its ability to conduct heat. It quantifies the rate at which heat energy is transferred through a material due to a temperature gradient. The higher the thermal conductivity of a material, the more efficiently it can transfer heat.

thermal conductivity indicates how quickly heat can move through a material when there is a difference in temperature across it. Materials with high thermal conductivity, such as metals, transfer heat rapidly, while materials with low thermal conductivity, such as insulating materials, transfer heat more slowly.

6.3.5.2- Specific Heat Capacity

Specific heat capacity, often simply called specific heat, is a physical property of a substance that measures the amount of heat required to change the temperature of a unit mass of the substance by one degree Celsius (or one Kelvin). Specific heat capacity indicates how much heat energy is needed to raise the temperature of a certain mass of a substance by a certain amount. Different substances have different specific heat capacities, which is why some materials heat up or cool down more quickly than others.

6.3.5.3- Density

Density is a physical property of a substance that measures the amount of mass contained in a given volume. It is a measure of how compact or concentrated a substance is. The units of density are typically kilograms per cubic meter (kg/m^3) or grams per cubic centimetre (g/cm^3). Density describes how much mass is contained in a given volume. A material with high density has a large amount of mass in a small volume, while a material with low density has a small amount of mass in a large volume. Density is an important property in various fields, including physics, engineering, and materials science, as it influences how substances behave and interact under different conditions.

6.3.5.4- Emissivity

Emissivity is a measure of a material's ability to emit thermal radiation relative to that of a perfect blackbody. It is a dimensionless quantity that ranges from 0 to 1, where:

- An emissivity of 1 corresponds to a perfect blackbody, which emits the maximum amount of thermal radiation possible at a given temperature.
- An emissivity of 0 corresponds to a perfect reflector, which does not emit any thermal radiation.

Emissivity depends on factors such as the material's surface properties, temperature, and wavelength of the emitted radiation. In practical applications, understanding emissivity is crucial for thermal management, designing radiative heat transfer systems, and interpreting

thermal imaging results. Materials with high emissivity are good emitters of thermal radiation, while those with low emissivity are poor emitters and often good reflectors.

6.3.6- Materials used in the project

The materials employed in this investigation were steel as described by EN1993-1-2 [38], gypsum as presented by EN1995-1-2 [39], the Rockwool used in the cavity insulation also presented by prEN1995-1-2 [39], cellulose [40] and cork [39]. These materials have an important impact in the numerical results.

6.3.6.1- Steel

The Figure 15 presents the thermal properties of steel. the specific heat of the carbon steels and it reaches 5000 [J/kgK] as the maximum heat this study is presented according to the EN1993-1-2 [38]

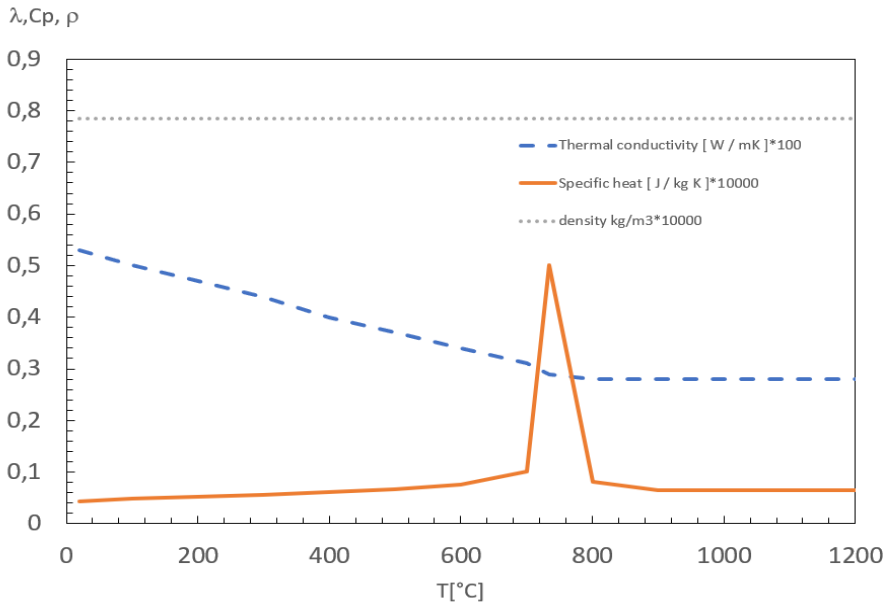

Figure 15: Thermal properties of steel[38].

6.3.6.2- Gypsum

The Figure 16 presents the thermal properties of gypsum. used in this study are presented according to the prEN1995-1-2 [39]. The specific heat of the plasterboard gypsum reaches 25000 [J/kgK] as maximum heat. Its Conductivity and its Density are also depicted.

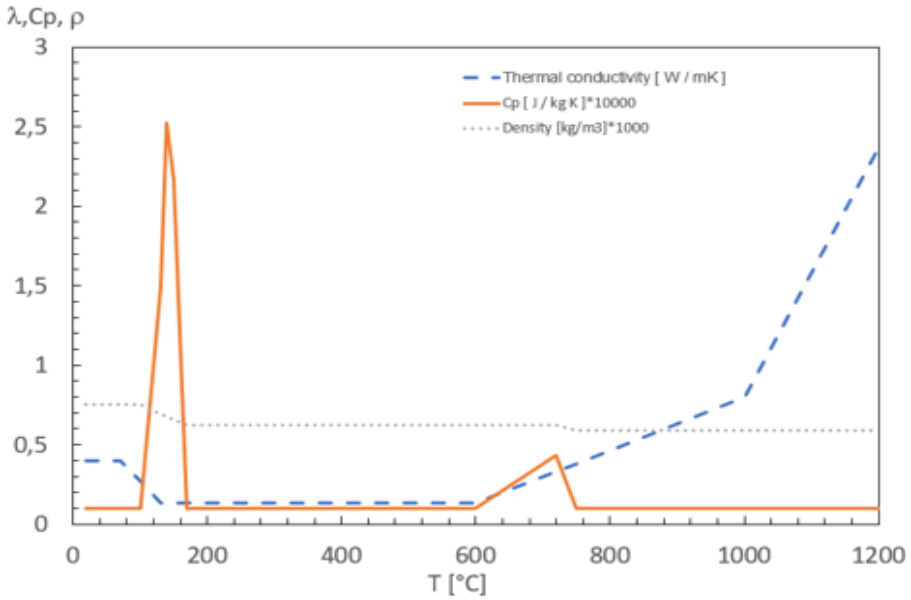

Figure 16: Thermal properties of Gypsum[39].

6.3.6.3- Rock-wool

The Figure 17 presents the thermal properties of rock-wool. The Rockwool [39] is the material used for the cavity and external insulation with density of 75 (kg/m3).

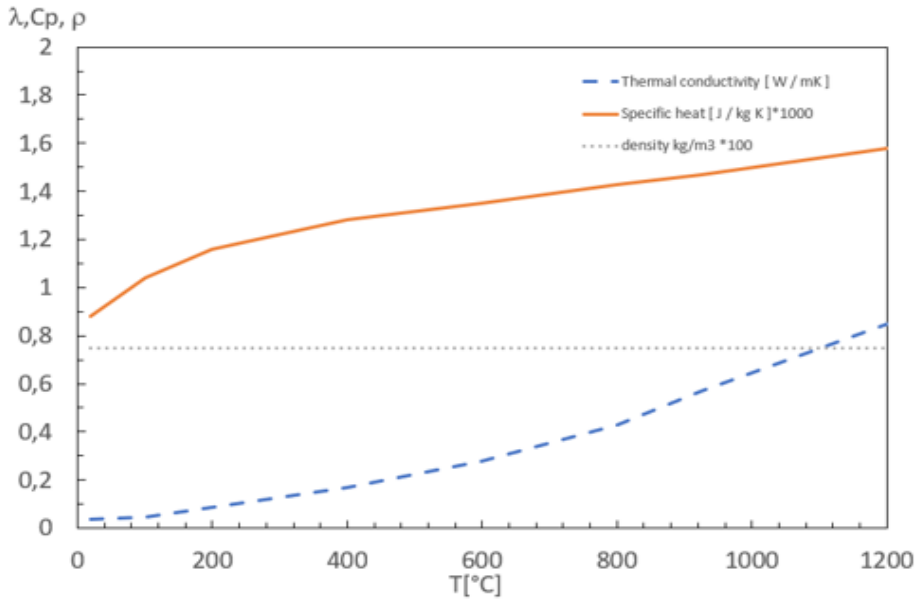

Figure 17: Thermal properties of Rock-wool[39].

6.3.6.4- Cellulose

The Figure 19 presents the thermal properties of cellulose[40]. The initial Cp value is 1000 J/kgK.. The Cp variation of cellulose insulation shows an initial peak value of 4500 J/kgK at 135°C.

Cellulose has excellent thermal insulation properties due to its ability to trap air pockets within its fibrous structure. It can help regulate indoor temperatures and contribute to energy efficiency in buildings.Cellulose is primarily made from plant sources, particularly from wood pulp. However, it can also be derived from other fibrous plants such as cotton, hemp, bamboo, and various types of grasses. The process typically involves breaking down these plant materials into cellulose fibers through mechanical or chemical means.

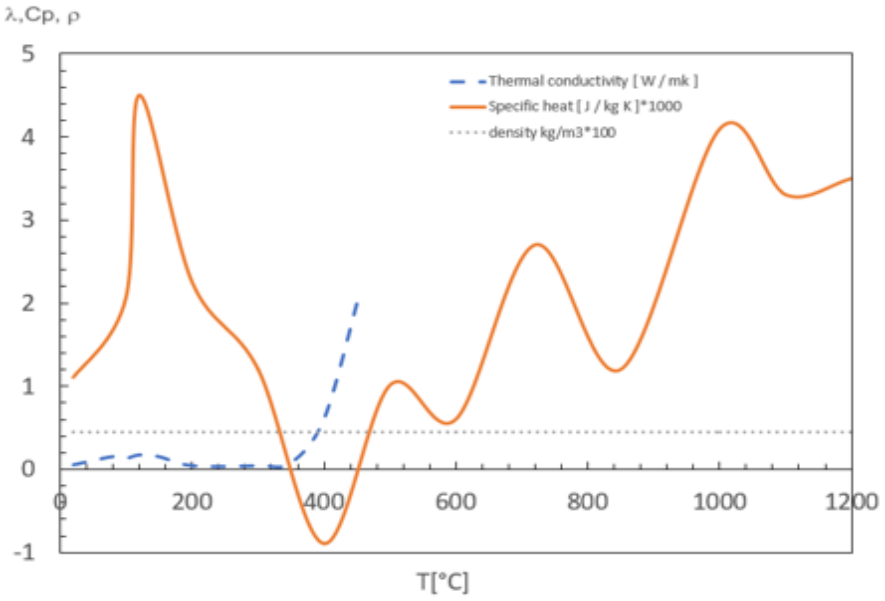

Figure 18: Thermal properties of Cellulose[40].

6.3.6.5- Cork

The Figure 19 presents the thermal properties of cork. These properties were adapted from wood. [39].

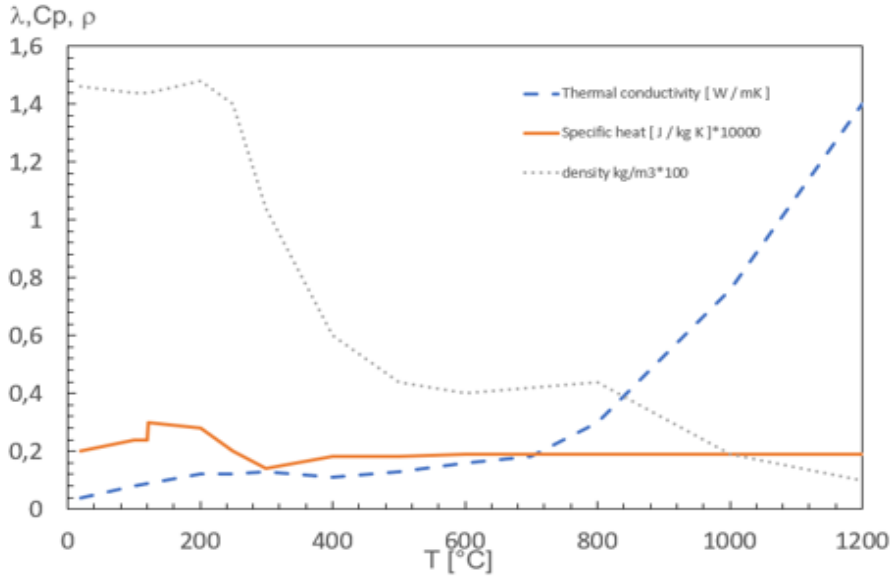

Figure 19: Thermal properties of Cork[39].

Chapter 7

7- NUMERICAL VALIDATION

All the specimens tested specimens were validated by the numerical models. Seven different specimens were selected from the tests developed by Paulo Piloto et al. [30] [31].

The accuracy of the models is evaluated by the RMSE (Root Mean Square Error) and Relative Error. The first error is evaluated by several time steps, comparing the measurements with the predictions and the second indicates that the numerical model provides a close approximation of the experimental findings regarding fire resistance.

7.1- Root Mean Square Error (RMSE)

RMSE, or Root Mean Square Error, is a statistical measure commonly used to evaluate the variance between predicted and observed values in a statistical model. It represents the square root of the average squared differences between predicted and observed outcomes and is mathematically the standard deviation of the residuals. Residuals denote the deviation between the model's predictions and the actual data points. In fire dynamics, RMSE is employed to compare experimental (observed) data with numerical (model-predicted) data, with the objective of minimizing its value. Lower RMSE values indicate a better fit of the model to the data and more accurate predictions, while higher RMSE values signify greater error and less accurate predictions in the model.

The equation for Root Mean Square Error (RMSE) is as follows:

$$\mathrm{RMSE} = \sqrt{\frac{1}{n}\sum_{i}^{n}(\mathrm{Texp} - \mathrm{Tnum})^2} \quad (10)$$

Where n represents the number of data points. To compare the numerical and experimental average temperature results, the RMSE equation is employed. The values reflect a good approximation, considering that, at any time, after the first 10 minutes of any standard fire test, the thermocouple temperature recorded by any furnace should not exceed more than 100 °C from the corresponding temperature of the standard temperature/time curve.

7.2- Relative error

The relative error of the difference between experimental and numerical test fire resistance (insulation) for Light Steel Frame (LSF) walls regarding TAVG (average temperature of the unexposed surface) and TMAX (maximum temperature of the unexposed surface).

$$\textbf{Relative Error} = \frac{\textbf{experimentalTAVG} - \textbf{numericalTAVG}}{\textbf{experimentalTAVG}} \quad (11)$$

Divide the absolute difference by the experimental value to get the relative error. This accounts for the magnitude of the difference relative to the size of the experimental value.

A low relative error indicates that the numerical model closely approximates the experimental results for the fire resistance, while a high relative error suggests significant discrepancies between the two.

7.3- Numerical Validation of all specimens

7.3.1- The validation of the Specimen 1

The Figure 20 presents the finite element mesh of the specimen 1. This specimen has 10815 elements and 11119 nodes defined.

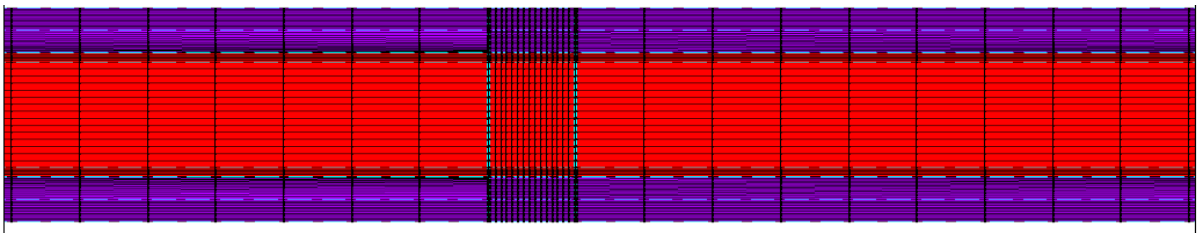

Figure 20: The finite element mesh of the specimen 1.

The Figure 21 presents the comparison between the experimental and numerical results for the temperature development in specimen 1.

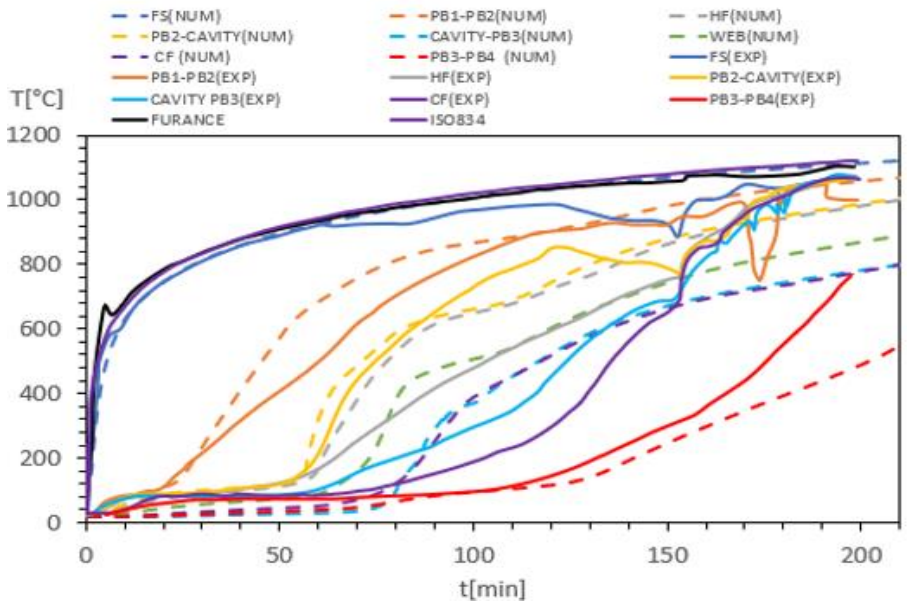

Figure 21: Average temperature results of specimen1

The Table 5 presents the RMSE between the predicted and observed temperatures of specimen 1.

Table 5: Results of (RMSE) of specimen1

FS (ºC)	PB-PB (ºC)	PB-CAVITY (ºC)	CAVITY-PB (ºC)	PB-PB (ºC)	HF (ºC)	CF (ºC)	WEB (ºC)
64	77	61	128	96	89	159	123

Figure 22 presents the average and the maximum temperature on the unexposed side in specimen 1.

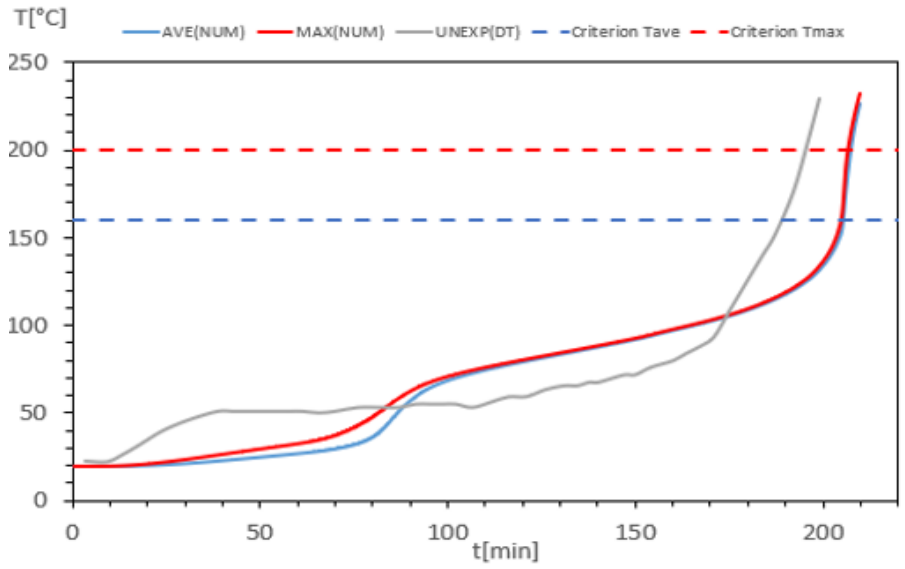

Figure 22: Average and maximum temperature on the unexposed side of specimen1.

The Table 6 represents Relative error for experimental and numerical tests of specimen1

Table 6: Relative error of specimen 1

Experimental Fire Resistance Tave (min)	**Numerical Fire Resistance Tave (min)**	**Relative Error (%)**
188	204	8,51

7.3.2- The validation of the Specimen 2

The Figure 23 presents the finite element mesh of the specimen 2. This specimen has 10659 elements and 11163 nodes defined.

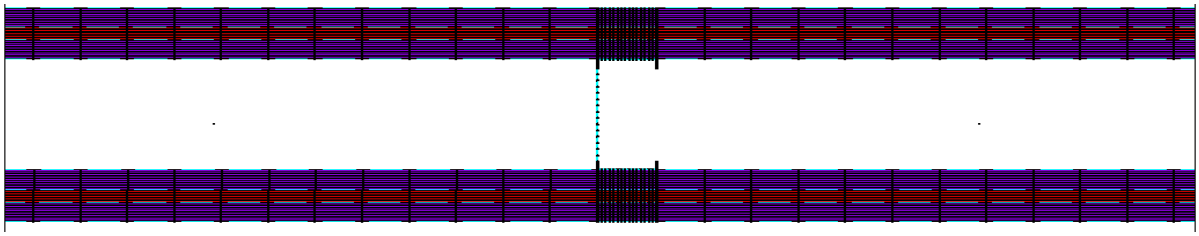

Figure 23: The finite element mesh of the specimen 2.

Figure 24 presents the comparison between the experimental and numerical results for the temperature development in specimen 2.

As we can notice in the figure there is a higher differences on the exposed side, and the reason of this justification is related to the material behaviour at higher temperatures lack of conductivity and density variation.

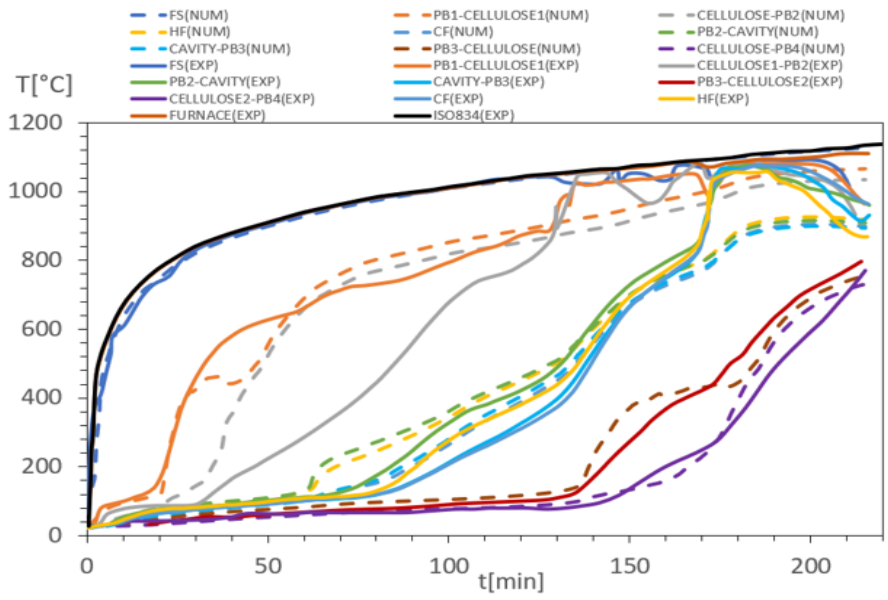

Figure 24: Average temperature results of specimen 2.

The Table 7 represents the RMSE between predicted and observed outcomes of specimen 2.

Table 7: Results of (RMSE) of specimen 2,

FS (ºC)	PB1-CEL (ºC)	CEL-PB2 (ºC)	HF (ºC)	CF (ºC)	PB-CAV (ºC)	CAV-PB3 (ºC)	PB3-CEL (ºC)	CEL-PB4 (ºC)
58	62	172	92	77	68	75	37	30

The Figure 25 presents average and maximum temperature on the unexposed side in specimen 2.

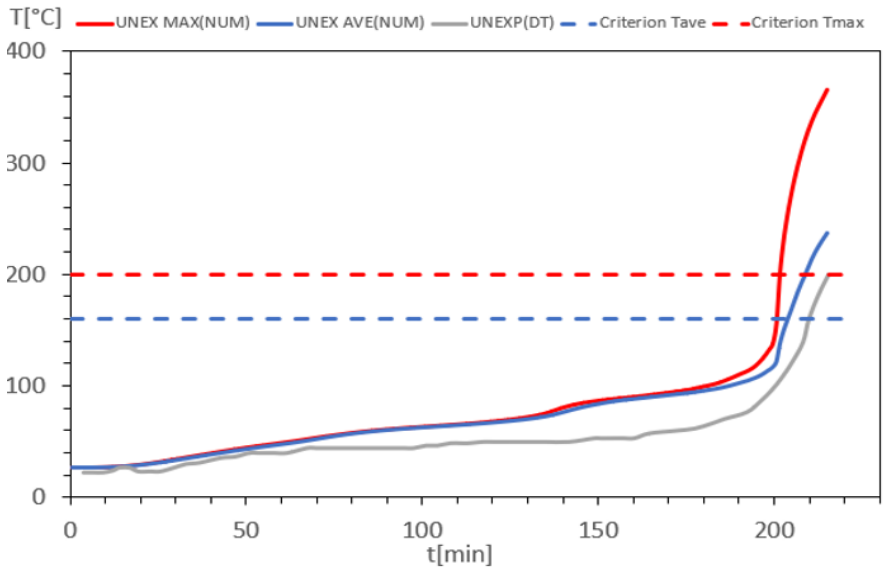

Figure 25:Average and maximum temperature
on the unexposed side of specimen 2

The Table 8 represents Relative error for experimental and numerical tests of specimen2

Table 8:Relative error of specimen 2

Experimental Fire Resistance Tave (min)	**Numerical Fire Resistance Tave (min)**	**Relative Error (%)**
204	211	3,43

7.3.3- The validation of the Specimen 3

The Figure 26 presents the finite element mesh of the specimen 3. This specimen has 6249 elements and 6441 nodes defined.

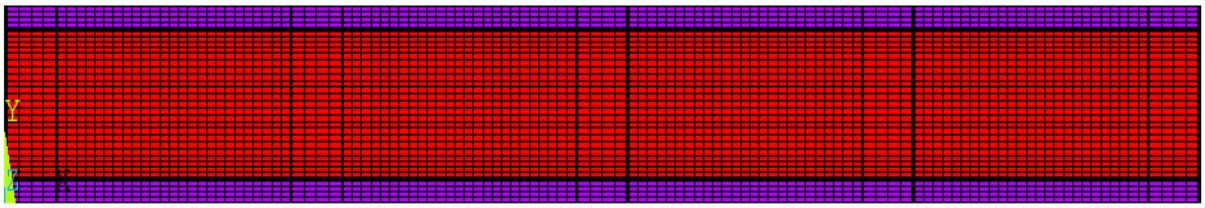

Figure 26:The finite element mesh of the specimen 3

The Figure 27 presents the comparison between the experimental and numerical results for the temperature development in specimen 3

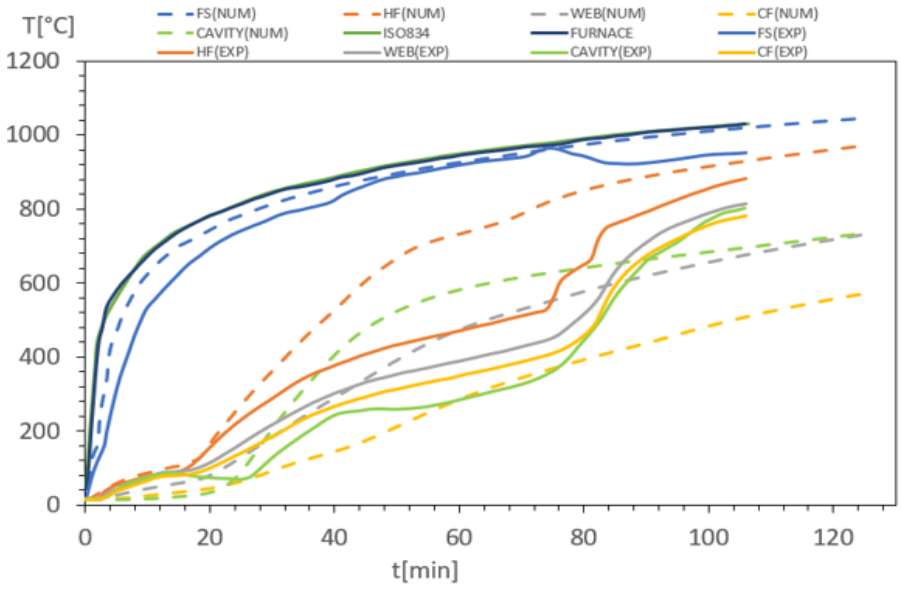

Figure 27:Average temperature results of specimen 3

The Table 9 presents the RMSE between predicted and observed outcomes of specimen 3

Table 9:Results of (RMSE) of specimen3

FS (ºC)	HF (ºC)	WEB (ºC)	CF (ºC)	CAVITY (ºC)
35	110	56	132	106

The Figure 28 presents the average and the maximum temperature on the unexposed side in specimen 3.

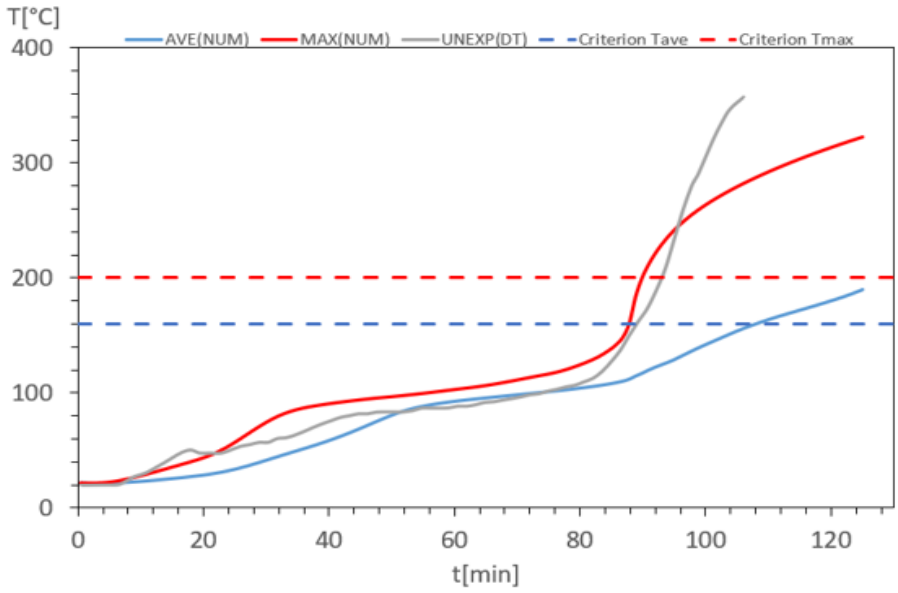

Figure 28:Average and maximum temperature
on the unexposed side of specimen3

The Table 10 represents the relative error for experimental and numerical fire resistance of specimen 3.

Table 10: Relative error of specimen3

Experimental Fire Resistance Tave (min)	**Numerical Fire Resistance Tave (min)**	**Relative Error (%)**
88	108	22.72

7.3.4- The validation of the Specimen 4

The Figure 29 presents the finite element mesh of the specimen 4

This specimen has 2700 elements and 3285 nodes defined.

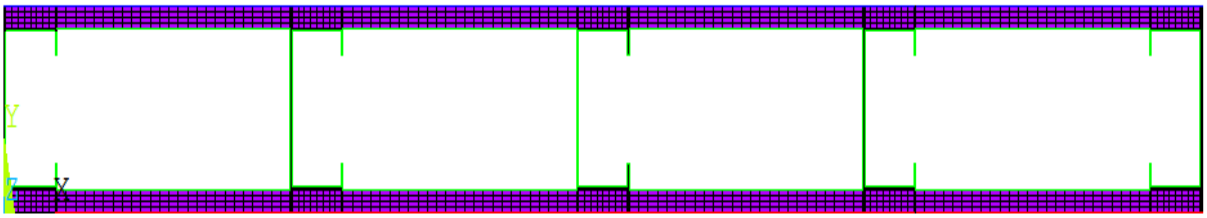

Figure 29:The finite element mesh of the specimen 4.

The Figure 30 presents the comparison between the experimental and numerical results for the temperature development in specimen 4

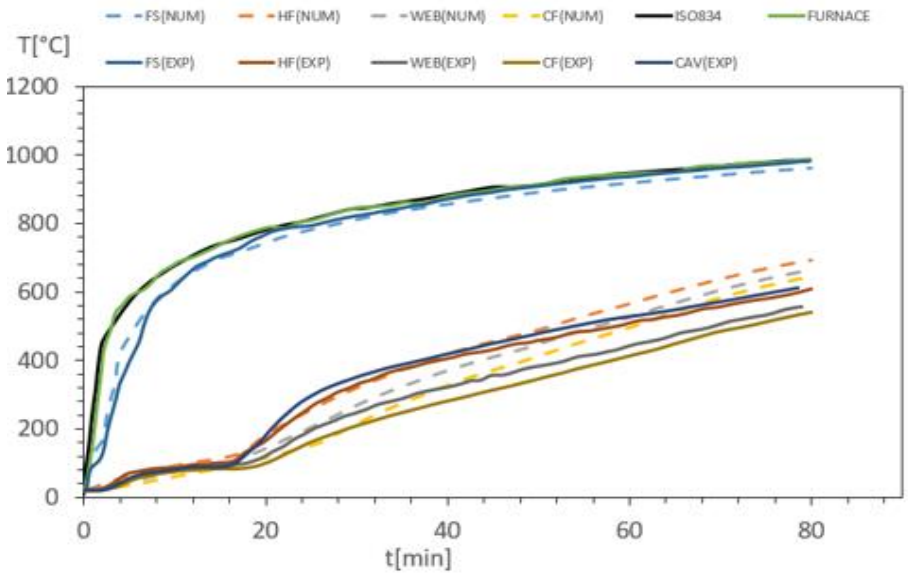

Figure 30:Average temperature results of specimen 4.

The Table 11 represents the square root of the average squared differences between the predicted and observed outcomes of specimen 4.

Table 11:Results of (RMSE) of specimen 4

FS (ºC)	HF (ºC)	WEB (ºC)	CF (ºC)
15	28	38	37

The Figure 38 presents the average and maximum temperature on the unexposed side in specimen4.

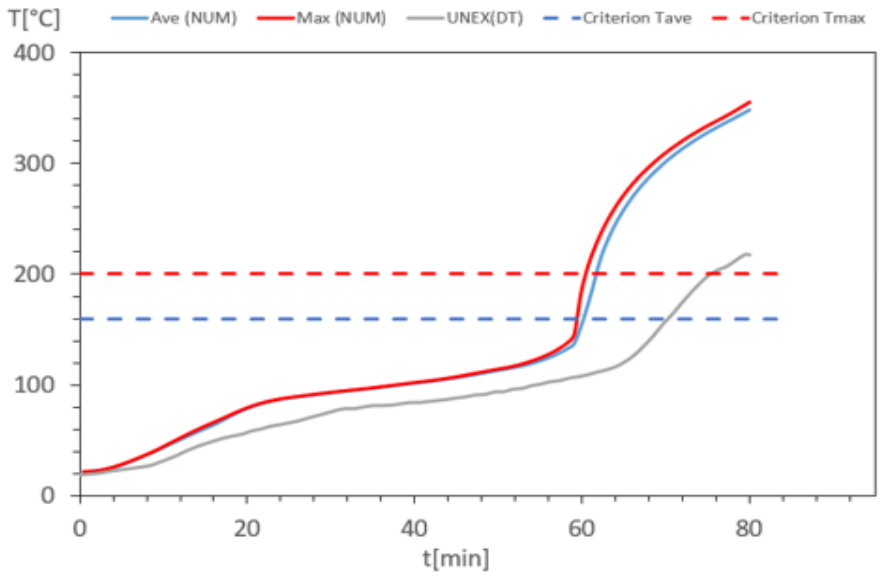

Figure 31:Average and maximum temperature
on the unexposed side of specimen4

The Table 12 presents the relative error between experimental and numerical results for the fire resistance of specimen4.

Table 12:Relative error for the fire resistance of specimen 4

Experimental Fire Resistance Tave (min)	Numerical Fire Resistance Tave (min)	Relative Error (%)
70	60	14,29

7.3.5- The validation of the Specimen 5

In this study, two methods will be utilized: the hybrid method and the interface element method (using LINK34 and LINK31 elements). These methods will be compared to determine the more effective approach by evaluating the Root Mean Square Error (RMSE) and relative error values. This comparison helps us to identify the best method for analyzing the fire performance of LSF walls. By analyzing these metrics, a thorough and precise evaluation can be ensured, ultimately improving the design and safety of these structures interface element method

7.3.5.1- The interface element method

The Figure 32 presents the finite element mesh of the specimen 5 using the interface element method linked with radiation and convection links

This specimen has 3531 elements and 3162 nodes defined

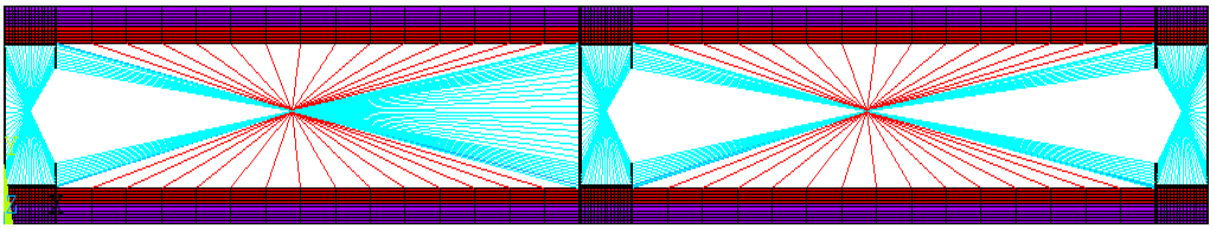

Figure 32:The finite element mesh of the specimen 5 using the interface element method

The Figure 33 presents the comparison between the experimental and numerical results for the temperature development in specimen 5

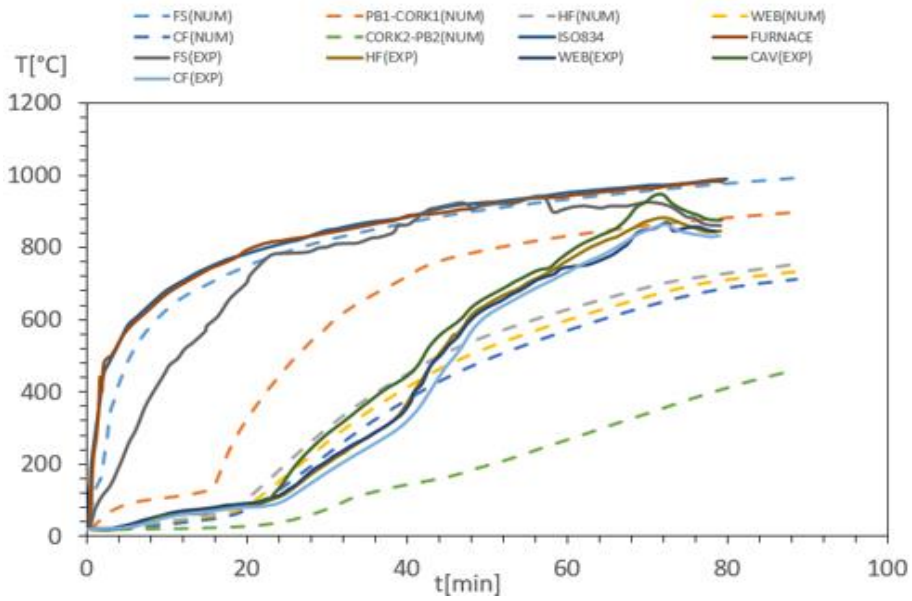

Figure 33:Average temperature results of specimen 5 using the interface element method

The Table 13 represents the square root of the average squared differences between predicted and observed outcomes for the controlling thermocouples of specimen5

Table 13:Relative error for the fire resistance of specimen 5 using the interface element method

FS (ºC)	HF (ºC)	WEB (ºC)	CF (ºC)
46	63	65	71

The Figure 34 presents average and maximum temperature on the unexposed side in specimen 5

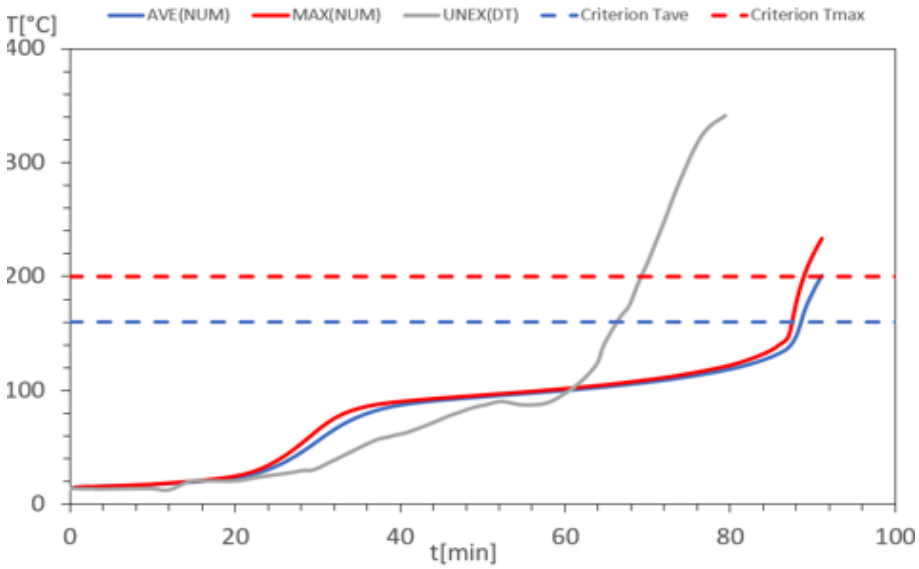

Figure 34:Average and maximum temperature
on the unexposed side of specimen5 using the interface element method

The Table 14 presents Relative error between the experimental and numerical results for the fire resistance of specimen 5

Table 14:Relative error of specimen 5 using the interface element method

Experimental Fire Resistance Tave (min)	**Numerical Fire Resistance Tave (min)**	**Relative Error (%)**
66	88	33,33

7.3.5.2- Hybrid method

The Figure 32 presents the finite element mesh of the specimen 5 using the hybrid method.

This specimen has 1944 elements and 2208 nodes defined.

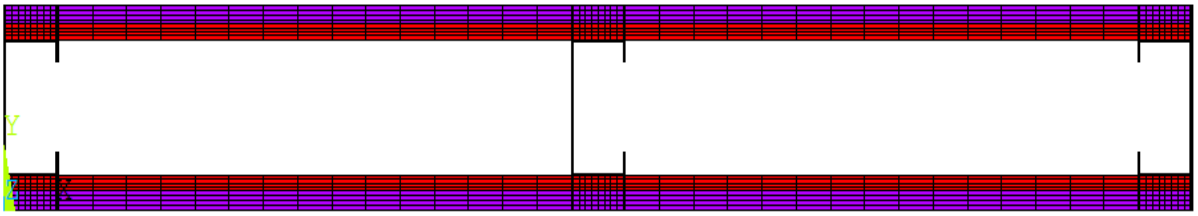

Figure 35: The finite element mesh of the specimen 5 using the Hybrid method.

The Figure 33 presents the comparison between the experimental and numerical results for the temperature development in specimen 5

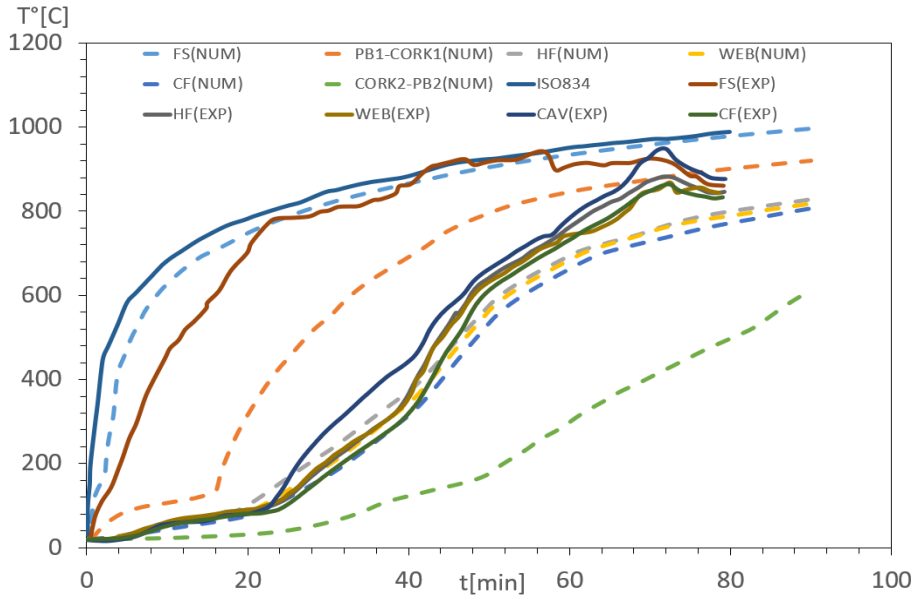

Figure 36: Average temperature results of specimen 5 using hybrid method.

The Table 13 represents the square root of the average squared differences between predicted and observed outcomes for the controlling thermocouples of specimen5

Table 15: Relative error for the fire resistance of specimen 5 using the Hybrid method.

FS (ºC)	HF (ºC)	WEB (ºC)	CF (ºC)
45	33	32	37

The Figure 34 presents the average and maximum temperature on the unexposed side in specimen 5

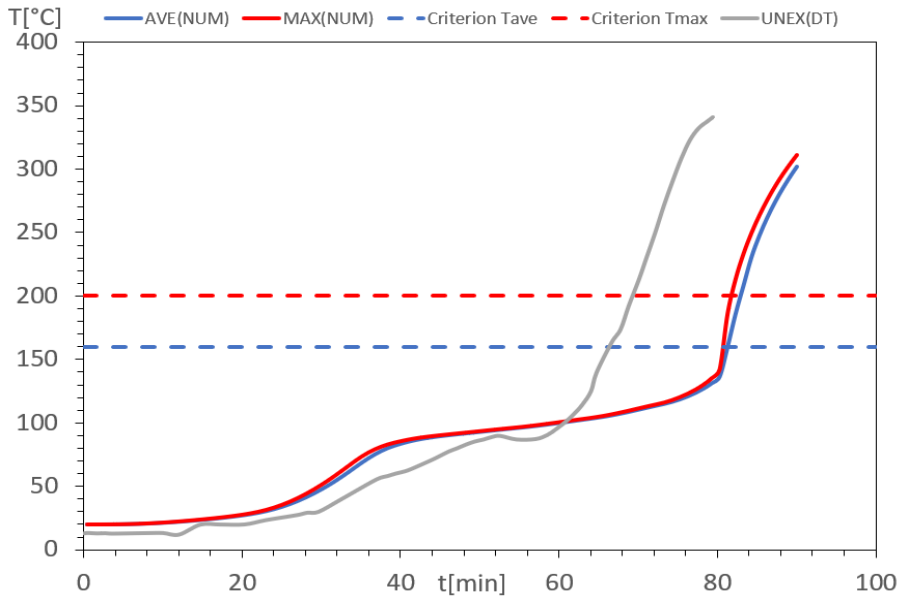

Figure 37: Average and maximum temperature on the unexposed side of specimen5 using the hybrid method

The Table 14 presents a relative error between the experimental and numerical results for the fire resistance of specimen 5

Table 16: Relative error of specimen 5 using the Hybrid method.

Experimental Fire Resistance Tave (min)	**Numerical Fire Resistance Tave (min)**	**Relative Error (%)**
65	81	24,62

7.3.5.3-Discussion of the Results for specimen 5

This study set out to determine the most effective modelling approach for accurately predicting the behaviour of the specimen by comparing two different methods: the hybrid method and the interface element method. Two sets of models were developed using Ansys ADPL, one employing the hybrid method and the other utilizing the interface element method. Both models were subjected to identical simulation conditions to ensure a fair comparison. Predicted values from each method were collected, and a detailed error analysis was performed, calculating the Root Mean Square Error (RMSE) and relative error for both methods.

The comparative analysis revealed that the hybrid method yielded significantly lower RMSE and relative error values compared to the interface element method. These results indicate that the hybrid method provides higher accuracy in modelling the specimen's behaviour. By integrating continuum and discrete models and combining various types of finite elements, the hybrid method leverages the strengths of different modelling approaches, resulting in more precise and reliable simulations.

The hybrid method has been identified as the superior modelling technique for this application, enhancing the reliability of the simulations and providing a robust framework for future modelling endeavours. This finding underscores the importance of using a comprehensive approach to achieve more accurate predictions in complex structural analyses.

7.3.6- The validation of the Specimen 6

The Figure 38 presents the finite element mesh of the specimen 6

This specimen has 3441 elements and 3815 nodes defined.

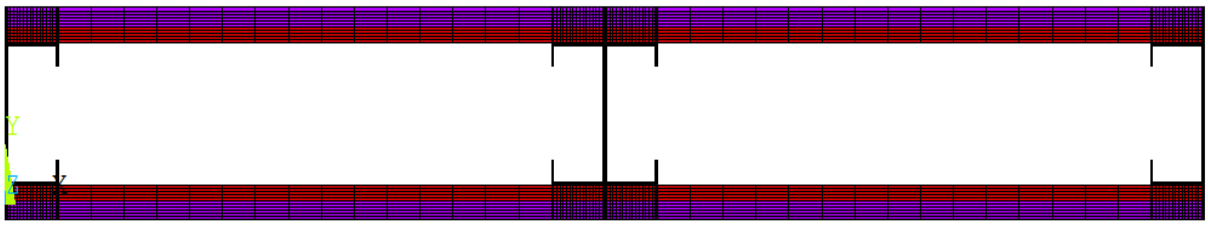

Figure 38:The finite element mesh of the specimen 6

The Figure 39 presents the comparison between the experimental and numerical results for the temperature development in specimen 6.

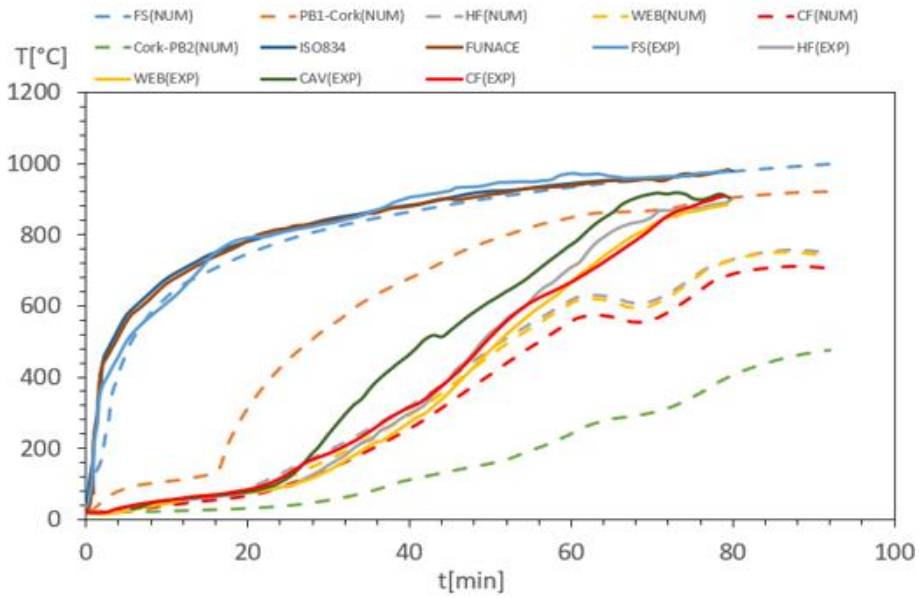

Figure 39:Average temperature results of specimen 6

The Table 17 presents the RMSE between the predicted and observed outcomes of specimen 6.

Table 17:Results of (RMSE) of specimen 6

FS (ºC)	HF (ºC)	WEB (ºC)	CF (ºC)
28	63	59	67

The Figure 40:Average and maximum temperature on the unexposed side of specimen6 presents the average and maximum temperature on the unexposed side in specimen 6.

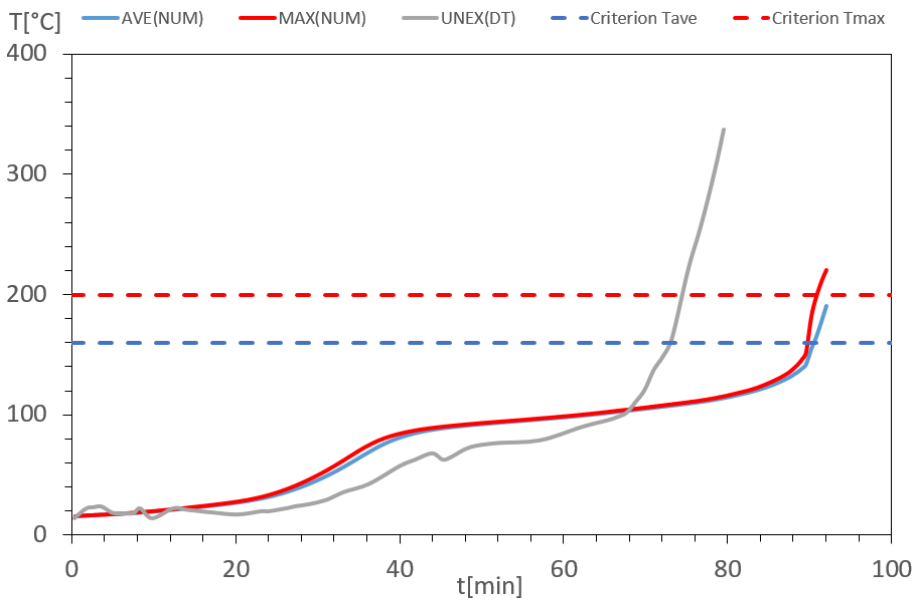

Figure 40:Average and maximum temperature
on the unexposed side of specimen6

The Table 18 represents the relative error between the experimental and numerical fire resistance test of specimen 6.

Table 18:Relative error of specimen 6

Experimental Fire Resistance Tave (min)	**Numerical Fire Resistance Tave (min)**	**Relative Error (%)**
73	90	23,29

7.3.7- The validation of the Specimen 7

The Figure 41 presents the finite element mesh of the specimen 7

This specimen has 2388 elements and 2827 nodes defined.

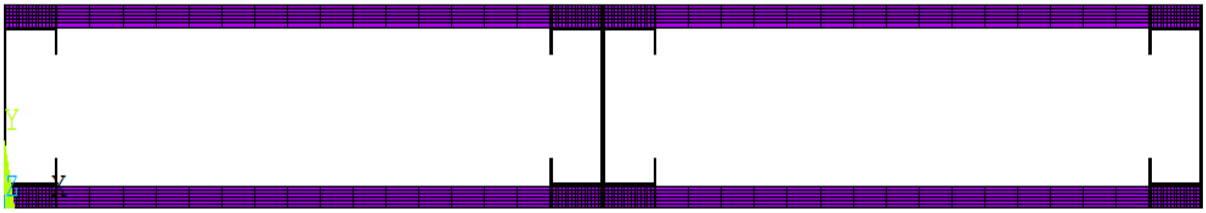

Figure 41:The finite element mesh of the specimen 7

The Figure 42 presents the comparison between the experimental and numerical results for the temperature development in specimen 7

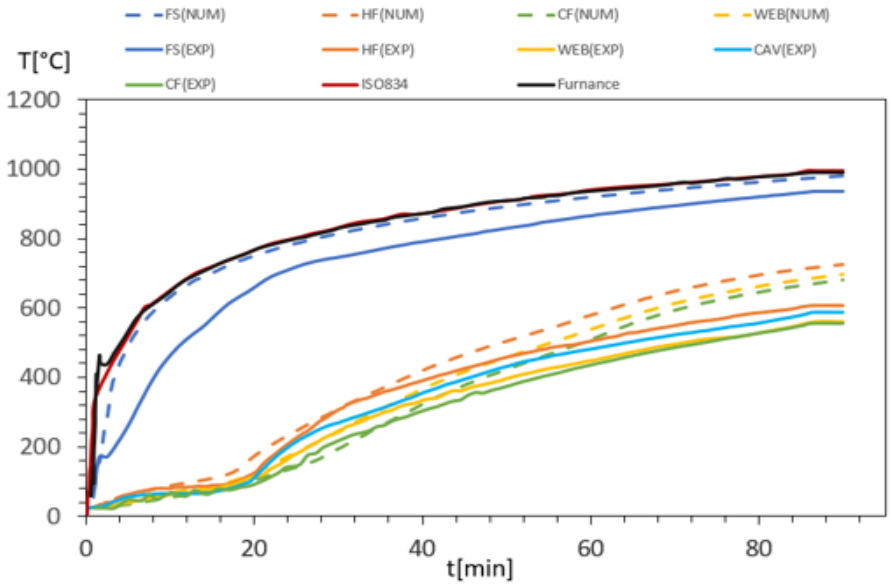

Figure 42:Average temperature results of specimen 7

The Table 19 presents the RMSE between the predicted and observed outcomes of specimen 7.

Table 19:Results of (RMSE) of specimen7

FS (ºC)	HF (ºC)	CF (ºC)	WEB (ºC)
49	36	38	43

The Figure 43 presents the average and maximum temperature on the unexposed side in specimen 7.

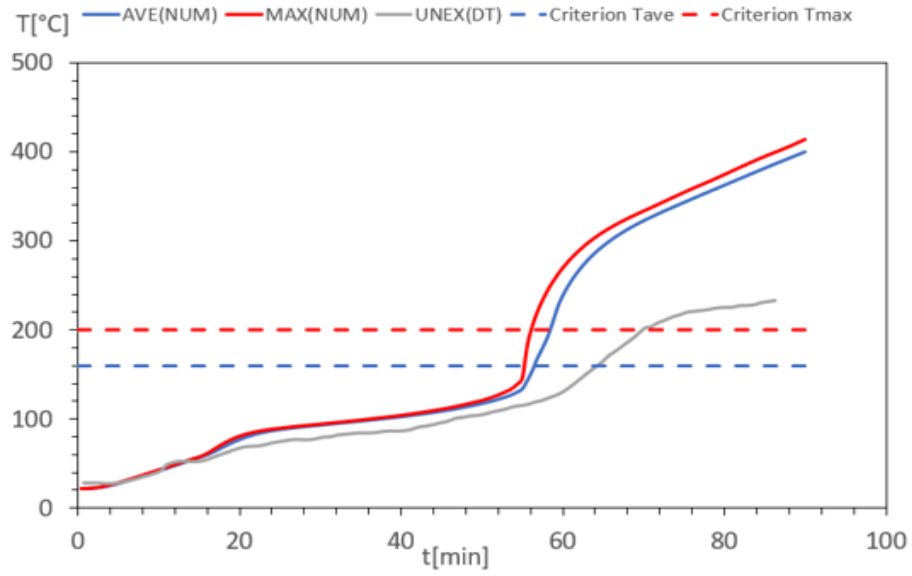

Figure 43:Average and maximum temperature
on the unexposed side of specimen7

The Table 20 represents Relative error for experimental and numerical fire resistance of specimen 7.

Table 20:Relative error of specimen 7

Experimental Fire Resistance Tave (min)	**Numerical Fire Resistance Tave (min)**	**Relative Error (%)**
64	56	12,50

7.3-Discussion of the Results

7.3.1- Impact of the position of insulation

This analysis examines the impact of insulation placement within Light Steel Framing (LSF) wall assemblies on fire resistance. Two specimens were compared: the first had cellulose insulation within the cavity, and the second had cellulose insulation sandwiched between two

layers of gypsum plasterboard, as can be seen in the Table . The objective was to determine which configuration provides better fire resistance.

Through the results of fire resistance time, it was found that the first specimen, with insulation positioned in the cavity, exhibited a longer fire resistance time compared to the second specimen. This indicates that the first configuration offers superior fire performance. These findings highlight the importance of optimal insulation placement to enhance the fire resistance and overall safety of building structures.

Table 21: Influence of the position of insulation

Specimen	Drawing	Position of insulation (cellulose)	Fire resistance (Tave)	Fire resistance (Tmax)
1	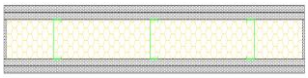	cavity	204	204
2	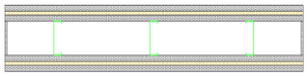	between two layers of gypsum	200	198

The specimen with cavity insulation demonstrated prolonged fire resistance, likely due to factors such as reduced thermal conductivity of cellulose, the presence of air gaps, and potential structural reinforcement offered by the cavity configuration. Conversely, the specimen with insulation between gypsum layers exhibited inferior fire resistance, despite benefiting from the thermal mass of gypsum.

7.3.2- Impact of adding cavity insulation

In this case, we investigate the influence of incorporating cavity insulation on the fire resistance of Light Steel Framing (LSF) walls. A comparison was made between two specimens: the first featuring rock wool insulation within the cavity, while the second had no insulation. By analyzing the fire resistance times of both specimens, it was observed that the first specimen, with cavity insulation, exhibited significantly longer fire resistance compared to the second. This underscores the crucial role of cavity insulation in enhancing the fire resilience of LSF wall assemblies. These findings emphasize the importance of integrating cavity insulation as a fundamental component of fire safety measures in building construction.

Table 22: Influence of adding cavity insulation

Specimen	Drawing	cavity insulation	Fire resistance (Tave)	Fire resistance (Tmax)
3	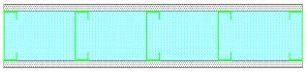	rockwool	106	88
4	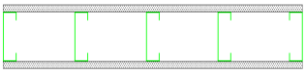	No	58	58

The test assessed the influence of cavity insulation, comparing a specimen with rock wool insulation to one without. Rock wool's low thermal conductivity slows heat transfer, prolonging fire resistance. Additionally, cavity insulation limits flame propagation and contains heat within the structure. As a result, the insulated specimen displayed markedly superior fire resilience compared to the uninsulated counterpart. These findings underscore the pivotal role of cavity insulation in bolstering building fire safety,

7.3.3- Impact of Stud Quantity and Spacing

We explore the Impact of Stud Quantity and Spacing through two cases. In the first case, we examine two specimens differing in stud quantity: one with 3 studs and the other with 4 studs.

These results are numerical. And If they are numerical the Tmax would be the same as we can see in the table Table 23

The analysis of fire resistance time revealed that the second specimen, equipped with 4 studs, exhibited a longer fire resistance duration compared to the first, indicating its superior performance.

Moving to the second case, we compare two specimens based on the spacing between studs. The first specimen features a smaller spacing between studs compared to the second. Evaluation of fire resistance time demonstrated that the first specimen outperformed the second, showcasing the importance of stud spacing in enhancing fire resilience. These findings emphasize the critical role of both stud quantity and spacing in determining the fire performance of LSF walls.

Table 23: Influence of Stud Quantity

Specimen	Drawing	Number of studs	Fire resistance (Tave)	Fire resistance (Tmax)
5	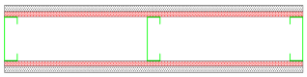	3	88	86
6	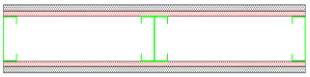	4	90	90

Increasing the number of studs in Light Steel Frame (LSF) walls can impact their fire resistance characteristics. The number of studs affects several key factors that determine how the wall system performs in a fire. In terms of fire resistance, the configuration and spacing of studs play critical roles. During a fire, steel conducts heat rapidly, and a higher density of studs can increase the potential for heat transfer through the wall. This thermal conductivity can affect the wall's ability to maintain its structural stability over time as the fire progresses. Design modifications, appropriate spacing, and effective fire protection measures are essential to ensure LSF walls meet regulatory fire safety standards and provide reliable protection in fire scenarios.

Table 24: Influence of Stud Spacing

Specimen	Drawing	Number of studs	Fire resistance (Tave)	Fire resistance (Tmax)
4	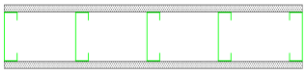	5	58	58
7	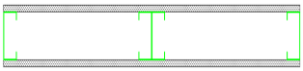	4	56	54

The reduced spacing means there are fewer gaps in the insulation layer, minimizing heat transfer pathways. This tighter arrangement may also contribute to better structural integrity by reducing the potential for buckling or deformation under heat stress.

7.3.4- Impact of the material and number of layers

In this analysis, we're exploring the influence of material composition and layering on fire resistance. We compared two specimens: the first featuring a dual-layer configuration of gypsum and cork, while the second had a single layer of gypsum. The results indicated that the fire resistance duration of the first specimen exceeded that of the second, suggesting its superior performance. This underscores the significance of both material choice and layering strategy in enhancing fire resilience.

Table 25: Influence of the material and number of layers

Specimen	Drawing	Plate layer(mm)	Fire resistance (Tave)	Fire resistance (Tmax)
6	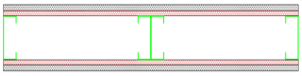	1 gypsum (12,5) 1cork(10mm)	90	90
7	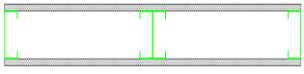	1 gypsum (12,5)	56	54

The superior fire resistance observed in the dual-layer configuration suggests cork's insulation properties enhance heat containment. Cork, known for its thermal stability and insulating abilities, likely slows heat transfer and delays temperature rise during a fire.

Chapter 8

8- CONCLUSIONS

In the thesis "Fire Insulation Performance of Non-Load Bearing LSF Walls," a comprehensive investigation into various factors influencing fire insulation performance has been conducted. The analysis of insulation position revealed that the location of insulation within the wall assembly significantly impacts its ability to withstand fire. Specifically, cavity insulation demonstrated superior fire resistance compared to other configurations, highlighting the critical role of insulation placement in enhancing fire resilience.

The incorporation of cavity insulation proved to be instrumental in improving fire resistance, as evidenced by the comparative analysis of specimens with and without cavity insulation. This emphasizes the importance of considering insulation materials and their positioning during construction to optimize fire safety measures.

The optimization of stud quantity and spacing emerged as another crucial aspect influencing fire insulation performance. By carefully adjusting the number and spacing of studs, it was possible to enhance thermal insulation, resulting in improved fire resistance.

The choice of material and the number of layers also significantly impacted fire insulation performance. The utilization of a hybrid method, which combines different modelling approaches, was found to be particularly effective in accurately predicting fire behaviour. This approach leveraged the strengths of various modelling techniques to provide more precise and reliable simulation results.

The importance of RMSE (Root Mean Square Error) and relative errors in validating numerical simulations against experimental data cannot be overstated. These metrics serve as critical tools for assessing the accuracy and reliability of simulation results, especially in complex engineering analyses such as fire insulation performance in non-load bearing LSF walls. In the context of fire insulation performance analysis RMSE and relative errors are vital in checking

if simulation models are accurate. By comparing these errors to set standards, researchers confirm the reliability of their results.

In conclusion, the thesis provides valuable insights into optimizing fire safety measures in non-load bearing LSF walls by considering factors such as insulation position, cavity insulation, stud quantity and spacing, material composition, and layering techniques. Through advanced numerical simulations and rigorous methodology comparisons, the study contributes to advancing fire safety standards in construction practices.

9- REFERENCES

[1] The American Iron and Steel Institute (AISI) "Design Guide for Cold-Formed Steel Purlin Roof Framing Systems".

[2] The Australian standard Cold–formed Steel Structures Code First published AS 1538–1974. Second edition 1988.

[3] Wei-Wen Yu, Roger A. LaBoube, Helen Chen Cold-Formed Steel Design

First published:1 October 2019 page 15

[4] Frances Maria Peacock Fire engineer report on the fire which occurred at a high-rise building in valencia, spain, on 22 february 2024 (Incendio de Valencia de 2024)

[5] Prof. G. Winter Effects of Cold-Straining on Structural Sheet Steels", by Alexander Chajes, S. J. Britvec, and G. Winter, J. of the Structural Div., ASCE, Page Vol. 89, No. ST2, April1963, pp. 1-32.

[6] The American Iron and Steel Institute (AISI) Web Crippling Behaviour of Cold-Formed Carbon Steel, Stainless Steel, and Aluminium Lipped Channel Sections with Web Openings.

[7] Prof. A. H. Chilver paper No 6495 structural problems in the use of cold-formed steel sections.

[8] Mehaffey and Cuerrier et al , “A model for predicting heat transfer through gypsum-board/wood-stud walls exposed to fire”, Fire and materials, vol. 18, no. 5, pp. 297–305, 1994.

[9] Y. Sakumoto et al. T. Hirakawa, H. Masuda, and K. Nakamura, “Fire resistance of walls and floors using light-gauge steel shapes”, Journal of Structural Engineering, vol. 129, no. 11, pp. 1522–1530, 2003.

[10] Prakash Kolarkar Structural and Thermal Performance of Cold-Formed Steel Stud Wall Systems under Fire Conditions, Queensland University of Technology, 2010.

[11] Gunalan et al. Green synthesized ZnO nanoparticles against bacterial and fungal pathogens Progress in Natural Science Materials International 22(6):693–700.

[12] Ayman Y. Nassif et al. Full-scale fire testing and numerical modelling of the transient thermo-mechanical behaviour of steel-stud gypsum board partition walls.

[13] S. Kesawan and M. Mahendran Post-fire Mechanical Properties of Cold-formed Steel Hollow Sections.

[14] Anthony Deloge Ariyanayagam, Mahen Mahendran esidual capacity of fire exposed light gauge steel frame walls.

[15] Dias et al. Article Predicting the fire performance of LSF walls made of web stiffened channel sections August 2018 Engineering Structures 168:320-332.

[16] Magarabooshanam et al. Article Fire resistance of non-load bearing LSF walls with varying cavity depth May 2020Thin-Walled Structures 150:106675.

[17] Tao et al. Fire tests and thermal analyses of LSF walls insulated with silica aerogel fibreglass blanket. Fire Safety Journal, 122, Article number: 103352.

[18] Gnanachelvam et al. Article Effects of insulation materials and their location on the fire resistance of LSF walls September 2021 Journal of Building Engineering 44(1):103323.

[19] Pancheti et al. Article Fire resistance of external LSF walls with corrugated steel cladding November 2021Journal of Constructional Steel Research 188(2).

[20] Perera et al. Article Fire performance of modular wall panels: Numerical analysis December 2021 Structures 34(2):1048-1067.

[21] Gardner et al Yun X. and Gardner L. Stress-strain curves for hot-rolled steel. Journal of Constructional Steel Research (2017) 133: 36-46. DOI: 10.1016/j.jcsr.2017.01.024.

[22] Rokilan and Mahendran. Effects of nonlinear elevated temperature stress-strain characteristics on the global buckling capacities of cold-formed steel columns.

[23] Piloto PAG, Khetata MS, Gavilan ´ ABR. Fire performance of non-loadbearing light steel framing walls - numerical simulation. In: in 7th international conference mechanics and materials in design; 2017. p. 1603–10.

[24] Khetata M, Fernandes L, Marinho C, Piloto P, Gavilan ´ A, Razuk H. “Fire resistance of non-loadbearing light steelframing walls: numerical validation”, in XI Portuguese Congress on Steel and Composite Construction –. CMM 2017, 2017,:853–62.

[25] Piloto PAG, Khetata MS, Gavilan ´ ABR. Fire Performance of Non-Loadbearing Light Steel Framing Walls-Numerical and simple calculation methods. MATTER Int J Sci Technol 2017;3(3):13–23.

[26] Mohamed Sultan M. A. Sultan, A model for predicting heat transfer through non insulated unloaded steel-stud gypsum board wall 414 assemblies exposed to fire, Fire Technology 32 (3) (1996) 239–259. doi:10.1007/BF01040217.

[27] Geoff Thomas Thermal Properties of Gypsum Plasterboard at High Temperatures June 2002 Fire and Materials 26(1):37 – 45.

[28] C. Ang and Y. Wang Article The effect of water movement on specific heat of gypsum plasterboard in heat transfer analysis under natural fire exposure September 2004 Construction and Building Materials 18(7):505-515.

[29] Keerthan P. and Mahendran Article Numerical studies of gypsum plasterboard panels under standard fire conditions October 2012 Fire Safety Journal 53:105–119.

[30] Piloto PAG’ Engineering Structures Contents lists available at Science Direct journal homepage: www.elsevier.com/locate/engstruct Engineering Structures 270 (2022) 114858.

[31] Piloto PAG’ International Journal of Thermal Sciences Contents lists available at ScienceDirect journal homepage: www.elsevier.com/locate/ijts International Journal of Thermal Sciences 193 (2023) 108511.

[32] International Organization for Stardardization, ISO 834-1 Fire-Resistance Tests - Elements of Building Construction Part 1: General Requirements, (1999).

[33] EN 1363-1, Fire resistance tests - part 1: General requirements. Brussels: European Committee for Standardization, 2020.

[34] EN 1364-1, Fire resistance tests for non-loadbearing elements. part 1: Walls. Brussels: European Committee for Standardization, 1999.

[35] EN 13501-2, Fire classification of construction products and building elements Part 2: Classification using data from fire resistance tests, excluding ventilation services

[36] EN.. 1991-1-2, Eurocode 1: Actions on structures - part 1-2: General actions - actions on structures exposed to fire. Brussels: European Committee for Standardization, 2002.

[37] APDL, ANSYS Mechanical. Mechanical applications Theory reference. ANSYS Release, 2010, vol. 13, no 010.

[38] EN (Belguim) 1993-1-2, Eurocode 3: Design of steel structures. part 1-2: General rules - structural fire design. Brussels: European Committee for Standardization, 2005.

[39] EN (Belguim) 1995-1-2, Eurocode 5 – design of timber structures. part 1-2: General – structural fire design. Brussels: European Committee for Standardization, 2004.

[40] Mahen Mahendran and Anthony Ariyanayagam research article Elevated temperature thermal properties of advanced materials used in LSF systems Accepted: 29 December 2020.

[41] Frances Maria Peacock Fire engineer report on the fire which occurred at a high-rise building in valencia, spain, on 22 february 2024 (Incendio de Valencia de 2024)